REPORT DOCUMENTATION PAGE

1. AGENCY USE ONLY (Leave blank)	2. REPORT DATE	3. REPORT TYPE AND DATES COVERED
		FINAL REPORT

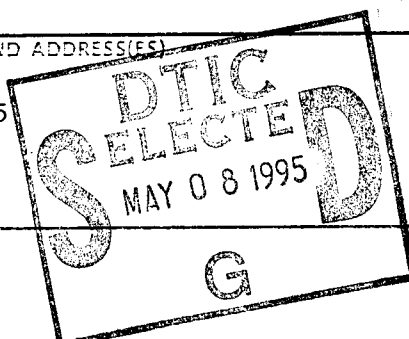**4. TITLE AND SUBTITLE**

Quantum and Nonlinear Optics Research

5. FUNDING NUMBERS

61102F
2301/BS

6. AUTHOR(S)

Prof Kaplan

7. PERFORMING ORGANIZATION NAME(S) AND ADDRESS(ES)

Dept of Electrical and Computer Engineering
Johns Hopkins University
Baltimore, MD 21218

8. PERFORMING ORGANIZATION REPORT NUMBER

AFOSR-TR· 9 5 - 0 3 2 9

9. SPONSORING/MONITORING AGENCY NAME(S) AND ADDRESS(ES)

AFOSR/NE
110 Duncan Avenue Suite B115
Bolling AFB DC 20332-0001

DTIC
ELECTED
MAY 0 8 1995
G

10. SPONSORING/MONITORING AGENCY REPORT NUMBER

AFOSR-90-0180

11. SUPPLEMENTARY NOTES

12. DISTRIBUTION/AVAILABILITY STATEMENT

APPROVED FOR PUBLIC RELEASE: DISTRIBUTION UNLIMITED

12b. DISTRIBUTION CODE

13. ABSTRACT (Maximum 200 words)

SEE FINAL REPORT ABSTRACT

19950505 170

DTIC QUALITY INSPECTED 3

14. SUBJECT TERMS	15. NUMBER OF PAGES
	16. PRICE CODE

17. SECURITY CLASSIFICATION OF REPORT	18. SECURITY CLASSIFICATION OF THIS PAGE	19. SECURITY CLASSIFICATION OF ABSTRACT	20. LIMITATION OF ABSTRACT
UNCLASSIFIED	UNCLASSIFIED	UNCLASSIFIED	UNCLASSIFIED

Final Technical Report

Grant AFOSR-90-0180

Quantum and Nonlinear Optics Research

Department of Electrical and Computer Engineering
The Johns Hopkins University, Baltimore, MD 21218
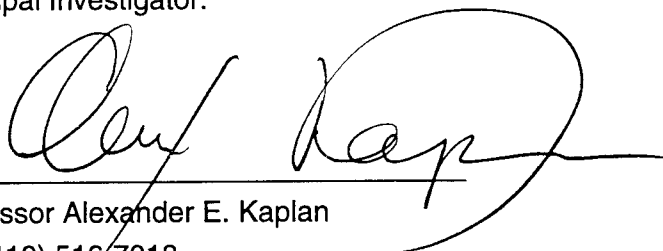
Submitted to

the U.S. Air Force Office of Scientific Research
Program Manager - Dr. Howard Schlossberg

Baltimore, Maryland
June 1994

Project Period: March 1, 1990 - February 28, 1993
(no-cost extension March 1, 1993 -- February 28, 1994)

Principal Investigator:

Professor Alexander E. Kaplan
ph. (410) 516-7018
FAX (410) 516-5566
e-mail sasha@super.ece.jhu.edu

Table of Contents

Accesion For		
NTIS CRA&I		☒
DTIC TAB		☐
Unannounced		☐
Justification		
By		
Distribution /		
Availability Codes		
Dist	Avail and / or Special	
A-1		

1. Brief overview of technical results

This grant was activated on March 1, 1990 with the project period of three years ending on February 28, 1993 (with no-cost extension March 1, 1993 -- February 28, 1994). The research of this principal investigator has continuously been supported by AFOSR from 1980. During that entire period under AFOSR support, the principal investigator authored or coauthored 212 publications, among them 5 book contributions, 68 regular journal papers, and 22 conference proceedings papers; the rest are conference papers.

In particular, under this AFOSR grant # 90-0180, more than 65 new papers have been published by this principal investigator and his research group, among them 15 papers in regular journals [1-15], 4 book contributions [16-19], 8 conference proceedings papers [20-27], and 32 conference papers [28-65].

Most of the proposed effects are novel and have initiated new opportunities in the field. The work by this principal investigator is highly credited by the research community in the field. Within the 1985-92, for example, his work was cited for more than 620 times (according to "Science Citation Index ") by other researchers (only those papers in which he was either the only or the first author, were counted). He has been a member of program committees and a panel member of several technical conferences on nonlinear optics and quantum electronics. He is an editorial board member of two international journals ("Optical & Acoustical Review" and "Nonlinear Optical Physics"). He was also a member of the Natl. Panel on "Math. for Material Sciences", 1991-92, and a member of ASAT US-USSR Laser Weapon Verification Meeting, June'91.

Since the research on this AFOSR grant started on March 1'90, a number of new results were obtained by this principal investigator and his group in the field of nonlinear optics and quantum electronics. The research progressed basically in these directions:

1.i.   Pilot theoretical research on X-ray nonlinear optics, including resonant saturation-related effects in plasmas (nonlinear absorption and nonlinear refractive index), and proposals for X-ray third harmonics generation, X-ray laser with noncoherent pumping, and X-ray four-wave mixing.

1.ii.   Experimental discovery and experimental and theoretical research on dark spatial solitons.

1.iii.   Theoretical investigation of previously discovered by this PI and his group dispersion-related multimode amplification, instabilities, oscillations and chaos in nonlinear counterpropagating waves.

1.iv.   Theoretical research on the fundamental problem of gradient-field-induced second-order nonlinear optical processing vacuum due to the photon-photon scattering of intense laser radiation in a dc magnetic field.

1.v. Collaborative (with Dr. Khurgin's group) theoretical and experimental research on non-linear optical effects (nonlinear refractive index, anomalous blue shift and bistability) in semiconductors.

1.vi. Other research

2. Technical reports on specific projects

2.i. Research on X-Ray Nonlinear Optics

In our research under this AFOSR grant, we explored opportunities for X-ray nonlinear optics based on the available X-ray lasers as potential quasicoherent sources and various plasmas as nonlinear media [7, 9, 10, 12, 14, 19, 23, 25, 26, 36, 46, 49, 50, 52-54, 56-58, 60-65]. The proposed effects include nonlinear refractive index effects, third-harmonic generation, four-wave mixing, and a proposal for a new X-ray laser pumped by a noncoherent X-ray pulse. This work was done by P. L. Shkolnikov and this P. I. The work on X-ray four-wave mixing was done in collaboration with P. L. Hagelstein and M. H. Muendel of MIT.

After the invention of optical lasers, nonlinear optics of visible domain has developed into one of the most important fields of optics with numerous applications to both science and technology. Now its shorter-wavelength counterpart, X-ray nonlinear optics with similarly great potentials and opportunities, is making its first steps. Although the very first publications on X-ray nonlinear optics (primarily about the parametric conversion of X-rays in solids) appeared in late 60's-early 70's, the entire field of X-ray nonlinear optics had to wait for X-ray lasers (XRLs) to come.

The first X-ray amplification was observed in 1984 at LLNL and PPPL. By now, more than fifty X-ray laser lines have been reported, with the wavelengths ranging from 326.5 Å down to 35.6 Å, with the output power up to several MW. Such rapid progress in XRL research revived interest in X-ray nonlinear optics. Apart from pure scientific interest (in particular, for X-ray laser spectroscopy), X-ray nonlinear optics also appears to have a great potential for applications to X-ray laser technology. A few X-ray nonlinear effects were preliminary considered in 1989 and 1990. A number of researchers working on X-ray lasers mentioned X-ray nonlinear optics as one of the most important future applications of X-ray lasers.

This principal investigator was among the first to realize importance and timeliness of X-ray nonlinear optics, and the first to propose full-scale research on the subject. Under this AFOSR grant, 19 papers have been published on the subject, among them 5 papers in regular journals [7, 9, 10, 12, 14], a book contribution [19], two conference proceedings paper [23, 25], and 11 conference papers (among them two invited [57,58]). Together with the early work, these results mark the birth of the theoretical X-ray nonlinear optics.

From the very beginning we realized that the main issue for X-ray nonlinear optics is not the theory of nonlinear propagation per se (which in its major features is substantially similar to that of visible domain), but the search for media in which X-ray nonlinear effects may be observed. Our very first estimations of X-ray nonlinearities showed that the main hope to achieve feasible effects at such short wavelengths, is to use *resonances*. We believe now that the entire business of X-ray nonlinear optics is about *resonant* couples, i. e. couples of XRL line + resonant transitions in a nonlinear media. From this point of view, plasmas turned out to be the first candidates to be considered as X-ray nonlinear media. That is because there are much larger selection of ionic spectra than that of neutral atoms. Indeed, Z-1 different degrees of ionization (that is, Z-1 different ionic spectra) are possible for an atom with the atomic number (nuclear charge) Z. Thus, if the total number of elements is Z_{max}, the total number of ionic spectra is $\sim Z_{max}^2/2$, i. e. more than 5000. Moreover, majority of ionic spectra consists predominantly of X-ray lines related to what may be called "Z-scaling". For example, the spectrum of a hydrogen-like ion (i. e. an ion with only one electron) with nuclear charge Z is roughly similar to the spectrum of the atomic hydrogen. The major difference is that all energies are scaled up by the factor of Z^2.

Thus, until now, our research interests have been concentrated on identification and estimation of couples "X-ray laser + plasma" resonant enough for the feasibility of various X-ray nonlinear effects. In the framework of our theoretical research on X-ray nonlinear optics, we have identified resonant nonlinear media (mainly plasmas) for about 1/3 of existing XRL lines. For these resonant media, we have also theoretically demonstrated the feasibility of several basic X-ray nonlinear optical effects such as

(i) nonlinear refraction and absorption saturation,

(ii) third-harmonic generation, and

(iii) four-wave mixing.

We believe that our results are promising enough to encourage experiments on X-ray nonlinear optics. We have also proposed

(iv) a new X-ray laser in Li vapor pumped by a short noncoherent X-ray pulse.

2.i.1. Saturation-related X-ray nonlinear effects in plasma.

Saturation-related X-ray resonant nonlinear effects in plasma were chosen by us to be considered first. The reason for that was that we wanted to use X-ray resonant nonlinearities inside an XRL itself. Our results suggested [7] that significant nonlinear change is feasible. For example, the output intensity of Se XRL line of 206 Å is much larger that the saturation intensity for the laser active medium. It may lead to an order of magnitude decrease in gain coefficient due to saturation. Furthermore, "nonlinear distance" turns out to be comparable to the length of the XRL active medium. [Here the "nonlinear distance" is the distance at which significant change in the phase front (up to 2π across the beam) may result from nonlinear

refraction].

Transition configuration used in XRL's is not very suitable when one wants to seek examples of coherent X-rays with separately prepared plasmas. Indeed, in the case of laser active medium, both of resonant levels are excited levels, and the lower level has to be populated, as it happens inside XRL's. Outside of an XRL's, both of them would be empty. Thus, to study nonlinear optics interactions of XRL radiation, it would be much more desirable to find much *cooler* plasmas , and with resonant ionic transitions from their ground (not excited) levels.

A plasma is a good candidate for saturation-related X-ray nonlinear effects if the resonant detuning $|\nu - \nu_0|$ between XRL frequency ν and frequency ν_0 of some transition from the ground to an excited level of the plasma ions, is smaller than the Doppler full width on half maximum of the respective plasma transition $\Delta\nu^D$. Search for such resonances is complicated by the lack of atomic information (wavelengths, oscillator and collisional strengths), especially on highly-ionized atoms. We have identified such resonant couples " XRL line + ion " for about one third of all the reported XRL lines (Table 1). As an example, we present our results for two X-ray lasers: Se and Ge (Table 2). The last column in the Table 2 contains the estimates of the "nonlinear length" $L_{NL} = \lambda/\Delta n^{NL}$ for given intensity $I = 5 \times I_s$ where I_s is the saturation intensity. One can readily see from Table 2 that nonlinear effects resulting from nonlinear refractive index can be observed at the Ge and Se XRL intensities even much lower than the intensities available now. The expected effects based on nonlinear refractive index are: self-focusing and "running foci" (although, because of significant probability of multiphoton processes, we do not expect a pronounced wave collapse, in contrast with the situation in liquids and solids); self-trapping of XRL radiation, self-bending and four-wave mixing. These effects may also be instrumental in direct measurement of nonlinear refractive index, plasma diagnostics, and for phase-conjugation amplification. It may also be possible that self- transparency and related 2π-solitons can be attained similar to that in the optical domain. The experimental observation of XRNE's in resonant couples of Table 2 is greatly facilitated by the fact that the required parameters T_e, N_e, and L of plasmas can be attained by using standard discharge devices.

	XRL $\lambda(Å)$	Plasma $\lambda_0(Å)$	$A(s^{-1})$	E_{ion} (eV)
1.	Ge^{22+} 236.26	Ar XIII 236.27	3×10^9	686
2.	Se^{24+} 220.28	Sc IV 220.280	6×10^8	73
3.	Se^{24+} 209.78	Fe X 209.776	1.3×10^8	262
4.	Se^{24+} 209.78	Cl XIII 209.81	10^{10}	656
5.	Ge^{22+} 196.06	Fe VII 196.046	4×10^{10}	125
6.	Ge^{22+} 196.06	Na III 196.054	1.8×10^9	72
7.	C^{5+} 182.173	Na IV 182.123	1.4×10^{10}	99
8.	Al^{10+} 105.69	Na IV 105.6867	2.4×10^{10}	99
9.	Al^{10+} 105.69	Cr VIII 105.69	4.3×10^{10}	185
10.	O^{7+} 102.355	Ni IX 102.340	1.9×10^{11}	193
11.	Eu^{35+} 71.00	Mg VIII 71.007	-	266
12.	Ta^{45+} 44.83	Si X 44.83	-	401
13.	W^{46+} 43.18	Cl IX 43.168	5×10^{11}	400

Table 1. Resonant couples "XRL radiation - plasma-ion transition". A denotes the corresponding transition probability, E_{ion} - the plasma ionization potential, λ and λ_0 - the wavelengths.

Couple	I (W/cm^2)	I^s (W/cm^2)	Δn^{NL}	L (cm)
1.	10^9	600	3×10^{-7}	6
4.	2×10^9	5×10^3	10^{-7}	18

Table 2. Saturation-related X-ray nonlinear effects in plasmas.

2.i.2. X-ray third-harmonic generation in plasmas of alkali-like ions

Absorption saturation and nonlinear refraction were our first research objects in X-ray nonlinear optics. Another, probably even more important effect, is higher-harmonic generation, since it is a method of choice to generate shorter-wavelength coherent radiation. Therefore, our next problem was to identify resonant media for X-ray third-harmonic generation [10].

(Since plasma is isotropic, the third harmonic is the lowest possible higher-harmonic, in the first-order approximation in velocities of free electrons and for not very strong optical field).

We face here the same problem of resonant coupling. But in this case the complication is in a sense tripled. Indeed, it is well known that the best resonant conditions for THG are the closest possible two-photon resonance and near (to a few linewidths, to avoid strong absorption) one- and three-photon resonances Strong optical coupling between levels of interest is also desirable. Because there is no tunable XRL available, one has to seek for plasmas that may allow for resonances to existing XRL lines. This search is complicated by insufficient information on energy levels and transition probabilities of ions. In this respect, plasmas of alkali-like ions present perhaps the best opportunity because of readily available atomic data. We have identified seven resonant couples for X-ray third-harmonic generation with plasmas on alkali-like ions (see Table 3).

To estimate conversion efficiency, we use standard results of the theory of THG in gasses and vapors, modifying them mainly to account for the specifics of the plasma dispersion. The X-ray refractive index due to free plasma electrons is $n_p(3v) \approx 1 - \omega_p^2/\omega^2$ where ω is the (angular) frequency of the incident XRL radiation, $\omega_p = (N_e e^2/\varepsilon_0 m)^{1/2}$ is the plasma frequency, and N_e is the plasma electron density. For all but one the couples "XRL line-plasma" in Table 3, this free-electron component of the refractive index is much larger than the resonant (bound-electron) one, which can therefore be neglected. In our estimates we also assumed that the plasma is homogeneous enough for us to neglect the refraction due to inhomogeneous electron distribution across the laser beam. As a result, the phase mismatch $\Delta k_p = 6\pi\lambda^{-1}[n_p(3\omega) - n_p(\omega)]$ where λ denotes the XRL radiation wavelength, is positive. The results of our calculations can be found in Table 3 in terms of the XRL intensities required to attain $C_{eff} \approx 10^{-8}$ (collimated beams assumed). They show that the observable THG intensities can be attained by available XRL's.

Resonant couples $\underline{XRL\ line\ \lambda(nm)}$ $plasma/E_{ion}(eV)$	$(\lambda/3)(nm)$	$I\ (W\ cm^{-2})$ for $C_{eff}=10^{-8}$	$\underline{Buffer\ ions}$ $\alpha/E'_{ion}(eV)$	$I\ (Wcm^{-2})$ for $C_{eff}=10^{-6}$
$\underline{Ge^{22+}\ 28.646}$ $K\ IX\ /176$	9.5487	8×10^{12}	-	-
$\underline{Se^{24+}\ 20.638}$ $Sc\ XI\ /250$	6.8793	2×10^{14}	-	-
$\underline{Se^{24+}\ 18.243}$ $Ne\ VIII\ /239$	6.0810	5×10^{12}	$\underline{Si\ VII}$ $0.06/247$	$2\times10^{11*}$
$\underline{C^{5+}\ 18.2097}$ $Ne\ VIII\ /239$	6.0699	2×10^{13}	$\underline{Be\ IV}$ $0.20/218$	10^{10}
$\underline{Y^{29+}\ 15.50}$ $V\ XIII\ /337$	5.167	2×10^{14}	-	-
$\underline{Ag^{37+}\ 9.93}$ $Al\ XI\ /442$	3.31	5×10^{14}	-	-
$\underline{Eu^{35+}\ 6.583}$ $Ga\ XXI\ /807$	2.194	2×10^{14}	$\underline{Ti\ XIV}$ $0.06/863$	7×10^{10}
$\underline{Na^{10+}\ 5.4194}$ $Cl\ XV\ /809$	1.8065	10^{15}	-	-

Table 3. X-ray THG in plasmas. α is the ratio of the required buffer ion density to the electron density, and E_{ion} and E'_{ion} are the ionization potentials of the "main" and "buffer" plasmas, respectively. The asterisk marks the result obtained for ion density $10^{18}\ cm^{-3}$.

(For example, the power of Ge^{22+} XRL required for $C_{eff}\approx10^{-8}$ in the loose focusing limit can be estimated as several MW which is close to the peak power of the existing XRL. It corresponds to the input energy of several hundreds of microjoules in a 100 ps pulse).

One of the ways to improve the X-ray THG is to facilitate ideal phase matching condition $\Delta k = 0$. Similarly to the optical THG, this can be done by adding a "buffer" medium or, in our case, buffer ions. Let some transition from the ground level of the buffer ions be resonant to the third harmonic, $\lambda/3 < \lambda_0$ where λ_0 is the central wavelength of the transition, and let no transition be in close resonance to the fundamental harmonic. Then the resonant refraction by buffer ions may compensate for free-electron phase mismatch if

$$1 - n_{buf}(3\omega) \approx 2\times10^{-3}(\lambda/3)(f/\Delta v^D)\,N'_i\,\overline{w}(x)$$

with the buffer ion density N'_i in cm^{-3} and λ in cm. Required plasma conditions may be

attained in some discharge devices. This way one can achieve several orders of magnitude enchancement. (For example, for C XRL, Ne VIII plasma as a nonlinear medium and Be IV as buffer ions the intensity required to attain $C_{eff} \approx 10^{-8}$ is four orders of magnitude smaller compared to unbuffered case.)

Our quantitative results should be viewed as preliminary estimates, in particular because at this stage some of the competing processes have been neglected. Nevertheless, we expect substantial third-harmonic intensities at the state of the art of both X-ray lasers and plasma technology. Further significant enhancement of the efficiency (up to several orders of magnitude for the same XRL intensity) require search for better resonant couples "XRL line-plasma".

2.i.3. X-ray laser frequency near-doubling and generation
of tunable coherent X-rays by four-wave mixing in plasma

Another third-order nonlinear effect, which may lead to X-ray laser frequency upconversion, is four-wave mixing of coherent X-ray and optical radiation [14]. One could expect high conversion efficiency for this process because (i) powerful optical lasers may be used; (ii) one of the participating frequencies is relatively low (optical); (iii) close resonances are more likely found. Moreover, this process may appear instrumental in generating tunable coherent X-rays.

We identify and evaluate plasmas in which efficient X-ray laser frequency near-doubling is expected for a number of available X-ray lasers by means of resonant four-wave mixing with Nd or KrF lasers. In some of these plasma, four-wave mixing of coherent X-rays and tunable optical radiation may result in tunable coherent X-ray radiation powerful sufficient for X-ray laser spectroscopy.

Of the various four-wave mixing processes, we have chosen to study difference-frequency mixing since in this case it seems relatively easy to attain optimal phase matching. As holds for X-ray nonlinear optics in general, only resonantly-enchanced effects may be observed at the present level of X-ray laser technology. We are therefore interested in resonant nonlinear media (plasmas) for the following difference-frequency mixing process:

$$\omega = 2\omega_{XRL} - \omega_{opt} \tag{A}$$

Here ω_{XRL} is the frequency of an XRL, and ω_{opt} is the frequency of an optical laser. For the purpose of XRL frequency near-doubling, we consider processes (A) with two particular optical lasers : a powerful Nd laser, which is used to pump most XRL's, or a very bright, short-pulse KrF laser. (In the latter case, the converted X-ray pulse duration may be much shorter than the duration of the incident X-ray pulse.) If a *tunable* optical laser is used instead, the result is tunable coherent X-ray radiation at almost doubled XRL frequency.

Ions of two isoelectronic sequences could be most useful for X-ray four-wave mixing. For many C-like ions, the energies of $2s^2 2p^2\ {}^3P - 2s2p^3\ {}^3P^o$ and $2s2p^3\ {}^3P^o - 2p^4\ {}^3P$ transitions are very close to each other, providing one with one- and two-X-ray-photon resonances.

Transitions from $2p^4\ ^3P$ levels to the nearest lower level $2s\,2p^3\ ^3S_1$ correspond to X-ray radiation if the previous two do, and therefore no three-photon resonances are possible for processes (A) in C-like ions. By the same token, tunable X-ray radiation may be generated in these ions through process (A) for a broad range of optical frequencies with good efficiency.

Na-like ions may provide all three resonances for processes (A). Also, the plasma temperature required for substantial presence of the Na-like ionization stage is relatively low due to low ionization potentials of Na-like ions. A disadvantage of Na-like ions as X-ray four-wave mixing nonlinear media is that initial levels of nonlinear transitions should be excited levels (only then are simultaneous one- and two-photon resonances possible), and it may be difficult to populate them significantly.

Resonant combinations of lasers and ions, with estimates of conversion efficiency, are listed in Table 4. The tight-focusing limit $b \ll L$ is assumed (b is the confocal parameter and L is the length of a plasma cell). To evaluate the minimum plasma length required, we make use of the feasible spot size $w \approx 2\ \mu m$ of the Y^{29+} 155Å XRL (confocal parameter $\approx 0.15\ cm$). Similar values of the confocal parameter are readily attainable for the Nd laser fundamental harmonic. We assume $b = 0.15\ cm$ for all the participating beams. It means that plasma length $L_{min} = 10\,b \approx 1.5\ cm$ satisfies the tight-focusing condition.

Medium E_{ion}	Lasers	K	λ	C_{eff}
1. Ar VIII 143 eV	Ge^{22+} 236.26Å– Nd 1.06 μm	3×10^{-53}	119.46 Å	*
2. K IX 176 eV	Se^{24+} 209.78Å– Nd 0.53 μm	10^{-52}	106.99 Å	*
3. Ca X 271 eV	Se^{24+} 206.38Å– Nd 0.53 μm	5×10^{-51}	105.24 Å	*
4. K IX 176 eV	Se^{24+} 206.38Å– Nd 0.266 μm	10^{-51}	107.35 Å	*
5. K IX 176 eV	C^{5+} 182.173Å– Nd 0.263 μm	3×10^{-56}	94.29 Å	*
6. Ca X 271 eV	Y^{29+} 155.0Å– Nd 0.5320 μm	10^{-54}	78.65 Å	*
7. V XIII 336 eV	Ag^{37+} 99.36Å– Nd 1.06 μm	10^{-53}	49.91 Å	*
8. Cu XIX 670 eV	Ta^{45+} 44.83Å– Nd 1.06 μm	4×10^{-56}	22.46 Å	0.01
9. Ca XV 894 eV	C^{5+} 182.097Å– KrF 0.2484 μm	10^{-53}	94.51 Å	*
10. Ar XIII 686 eV	Se^{24+} 209.78Å– KrF 0.2484 μm	6×10^{-57}	109.51 Å	0.03

Table 4.   X-ray laser frequency near-doubling by four-wave mixing with optical laser in plasma.
* denotes conversion efficiency near 1 (with competing processes neglected).

In order to improve phase matching, the product $|b\,\Delta k|$ should be made as small as possible. For collinear beams with fixed confocal parameters, this can be done by adjusting of the electron density. For example, for assumed $b = 0.15\,cm$ and $\lambda_2 = 2.484\times10^{-5}\,cm$ (KrF laser), $b\,\Delta k \approx -1$ for $N_e \approx 10^{18}\,cm^{-3}$. It yields $|F_2|^2 \approx 4$ which is only two times smaller that the optimal value of 8 (for zero phase mismatch $\Delta k = 0$).

For the sake of uniformity, all the values of C_{eff} listed in Table 4 are estimated for $N_e = 10^{18}\,cm^{-3}$ and $|F_2|^2 \approx 4$. Our quantitative results should be viewed as only order-of-magnitude estimates, largely because at this stage we neglected all the competing processes. (It is worth noting , however, that substantial photoabsorption is unlikely to occur for all the cases considered, due to relatively low density and small length of plasma, and due to the absence of close resonances.) Nonetheless, these estimates allow one to expect substantial output power at almost doubled frequency for a number of available XRL's.

Tunable X-ray radiation may result from four-wave mixing (A) with tunable optical lasers. In particular, a tunable laser with the wavelength near 5000 Å and the power P_2 would produce broadly tunable output $P \approx 10^{-5}\times P_2$ at almost doubled XRL frequency by mixing with C^{5+} XRL in Ca XV plasma or with Se^{24+} 209.78Å XRL in Ar XIII plasma (from lines 9 and 10 of Table 4, respectively). For P_2 of a few MW, converted power of tens of watts which may be sufficient for the purposes of X-ray linear spectroscopy.

2.i.4. Proposal for 19.9 nm laser in Li pumped by a noncoherent X-ray pulse.

All X-ray lasers reported to date operate in hot and dense plasma which requires very high pumping power and results in broad ($\sim 10^{-4}$) bandwidth of amplified X-rays. A variety of pumping schemes have been proposed for the last three decades to attain X-ray lasing in a cold medium. Most of them rely on removal of atomic inner electrons by either noncoherent X-rays or by electron impact. An X-ray laser pumped through inner-shell photoionization, however, has not been realized yet. One of the main obstacles to proposed lasing to the ionic ground level [49] has been that such pumping would create free electrons energetic and numerous enough to destroy population inversion by electron-impact ionization of neutral atoms.

We have theoretically demonstrated [12] how the problem of 19.9 nm lasing on the $1s\,2p - 1s^2$ transition in Li^+ pumped by the inner-shell photoionization and photoexcitation on neutral Li atoms, can be solved. To limit the detrimental effect of the photoelectrons created by the pumping radiation, on the population inversion, we suggest making use of a short soft-X-ray pulse with a narrow-band spectrum centered at the Li $[1s\,(3s\,3p)\,^3P]\,^2P^o$ resonance to excite ground-state Li atoms. Subsequent fast autoionization of part of the inner-shell excited Li atoms to the upper laser level ($Li^+\,1s^22p\,^1P$) is complemented by the direct 1s-photoionization of Li atoms to the upper laser level. Suggested pumping scheme relies upon the relatively large both photoabsorption cross-section and the probability of the inner-shell (auto)ionization to the $Li^+\,1s\,2p\,^1P$ state in the vicinity of g resonance of neutral Li (≈ 71 eV above the ground level). At the same time, our calculations show that the energy distribution of emerging photoelectrons does not allow them to significantly destroy the population inversion. The spectral intensity of the short pumping pulse required to attain significant gain seems feasible at the the state of the art of the laser-plasma technology. It is also possible that much lower X-ray pulse spectral intensity may be required to pump the *excited* Li atoms by a broadband short X-ray pulse.

It is well known that the absorption of soft X-ray radiation (the photon energy in the region 57-100 eV) by Li atoms may produce double-excited states with energies much higher than the 2s-ionization potential of 5.39 eV of neutral Li. A Li atom in many of these states is unstable against autoionization: within a very short time (10-100 ps) it emits a free electron whereby turning into a Li^+ ion in one of the excited states.

Double-excited autoionizing Li atomic states correspond to broad resonances in the photoabsorption spectra of Li vapor for the energy of the incident photons above 58 eV. For the incident photon energy large enough to ionize a ground-state Li atom to the $Li^+\,1s\,2p\,^1P$ state, the strongest such a resonance corresponds to the $[1s\,(3s\,3p)\,^3P]\,^2P^o$ (71.14 eV above the Li ground level) state of Li atoms. The energy interval between $E' = 71.05$ and $E'' = 71.25 eV$ approximately corresponds to the width of this resonance. Absorption of a photon with such energy would immediately result in either (i) excitation of Li atom to the

$[1s\,(3s\,3p)\,^3P\,]\,^2P^o$ state followed by the autoionization to one of the four ionic state: $1s\,2s\,^1S$, $1s\,2s\,^3S$, $1s\,2p\,^1P$, and $1s\,2p\,^3P$, and by freeing of an electron with the energy of approximately 5.0 eV, 6.7 eV, 3.5 eV, or 4.5 eV, respectively; or (ii) direct (nonresonant) inner-shell ionization to the same ionic and photoelectron states; or (iii) 2s-ionization i. e. creation of a Li^+ ion in the ground $1s^2$ state and a free 65.7 eV-electron.

The process (iii) creates ground-state Li ions whereby decreasing the population inversion. However, the 2s-photoionization cross section is very low for the photon energy so high above the 2s-ionization potential of 5.39 eV. As a result, Li^+ ground level population due to the direct 1s-photoionization does not exceed 0.013 of the population of the ionic excited levels and may be neglected.

Processes (i)-(iii) are directly initiated by the pumping radiation. In turn, they bring about a variety of secondary processes. We have evaluated the most important of them: a) the 2s-ionization of Li atoms by electron impact (which has been considered as the main danger to the population inversion); b) collisional and optical transitions from the upper laser level to levels other than the lower laser level; c) the electron-impact excitation of the ground-state Li atoms. Out calculations show that all these processes would hardly diminish the inversion significantly: before substantial amount of Li atoms could be ionized by photoelectrons, almost all of these electrons would lose their energy through the collisional excitation of the ground-state Li atoms to the $1s^2 2p$ level (process c)), due to very large cross section of this process.

Estimated pumping intensity seems moderate. For instance, incident noncoherent X-ray spectral intensity required to attain gain-length product of ≈ 10 in a traveling-wave design, is radiated by 105 eV black body. Such a temperature is readily attainable in laser-produced plasma (one may compare this temperature with $\sim 1500\ eV$ temperature of existing X-ray laser active media).

For considered pumping by the 1s-photoionization of Li atoms from their ground state $1s^2 2s$, the probability of the ion to be left in the 1s2p configuration is significantly smaller than in the 1s2s configuration. Only in the vicinity of $[1s\,(3s\,3p)\,^3P\,]\,^2P^o$ resonance, this proportion changes somewhat to favor 19.9 nm lasing. As a result, such lasing would require narrow-band pumping. However, some recent experimental results on the soft-X-ray inner-shell ionization of another alkali, Na, allow us to suggest that the proposed 19.9 nm X-ray laser in Li may be efficiently pumped by photoionization of *excited* $1s^2 2p$ Li atoms with a short X-ray pulse of a much broader spectrum. We are going to consider such pumping in more detail later.

2.i.5. New subjects in X-ray nonlinear optics

Close to the end of this grant period, we began research along a new line in X-ray nonlinear optics, with the intent to explore it in detail under our continued (current at this point) AFOSR grant. This new research is related to the recently discovered nonlinear effect -- very

high order harmonic generation of optical lasers, with the highest harmonics reaching into soft-X-ray domain. We started exploring *new* nonperturbative mechanism of this process, the so called super-driven two-level atom [27,60,64,65]. We also began research on optimal phase-matching conditions for frequency upconversion of optical laser radiation into X-ray domain in plasma [63]. Our detailed results on this new subjects which were obtained under current (at this point) AFOSR grant have been published in a few journal papers.

2.ii. Spatial Dark Solitons in Self-Defocusing Materials

In our research, a new phenomenon of spatial dark solitons (SDS) have been experimentally discovered and theoretically explained [1,4,24, 31, 38, 41, 42, 47, 48, 51, 55, 59]. The dark solitons appear as stable, nondivergent stripes and grids in the transverse plane of a laser beam that passes through a rectilinear diffraction screen before propagating in a self-defocusing nonlinear material. Materials with different mechanisms of nonlinearity manifest the same qualitative results. The SDS nature of the observed phenomenon was verified by numer-ical simulations of the (2+1)-D nonlinear Schrödinger equation, analytical solutions for the (1+1)-D case, and their comparison with experimental data. This work was done by this PI's research group (including G. A. Swartzlander Jr. and H. Yin) in collaboration with Dr. D. R. Andersen of the University of Iowa and his group.

Dark solitons have provoked much interest since they were first shown to be particular solutions of the two-dimensional (1+1)-D nonlinear Schrödinger equation (NSE) with a negative (self-defocusing type) nonlinear coefficient n_2 (see Eq. (1) below). As opposed to a so-called "bright" NSE soliton, which propagates as a stationary wavepacket of finite extent in a (1+1)-D nonlinear medium with $n_2>0$, a "dark" soliton is characterized as a stationary "hole" on an oth-erwise uniform plane wave -- it exists on a background field as an absence of energy in a local-ized region, with constant size and shape parameters, and remarkable stability.

So far, only (1+1)-D *temporal* dark solitons (i. e. intensity minimums propagating along a nonlinear fiber on a quasi-cw bright background) have been observed experimentally. We observed stable *spatial* structures (e. g., stripes, crosses and grids) in the transverse cross-section of a cw optical beam propagating in a material with a self-defocusing nonlinearity, with these structures having a strongly pronounced soliton nature -- namely that of spatial dark soli-tons (SDS's). Although no (2+1)-D analytical solution for dark solitons in the NSE is known to date, our experimental and numerical data with various 2-D amplitude and phase masks pro-vided strong evidence that the phenomenon observed by us is indeed due to spatial dark soli-tons. Furthermore, our results on quasi-(1+1)-D propagation (see also [1]) have shown excel-lent agreement with the well known analytical results for (1+1)-D dark solitons.

In comparison to temporal solitons, SDS's are easy to create and observe experimentally, requiring as little as a HeNe laser and some slightly absorbing fluid. Various applications of SDS's can be envisioned, such as optical encoding, limiting, switching and computing, and
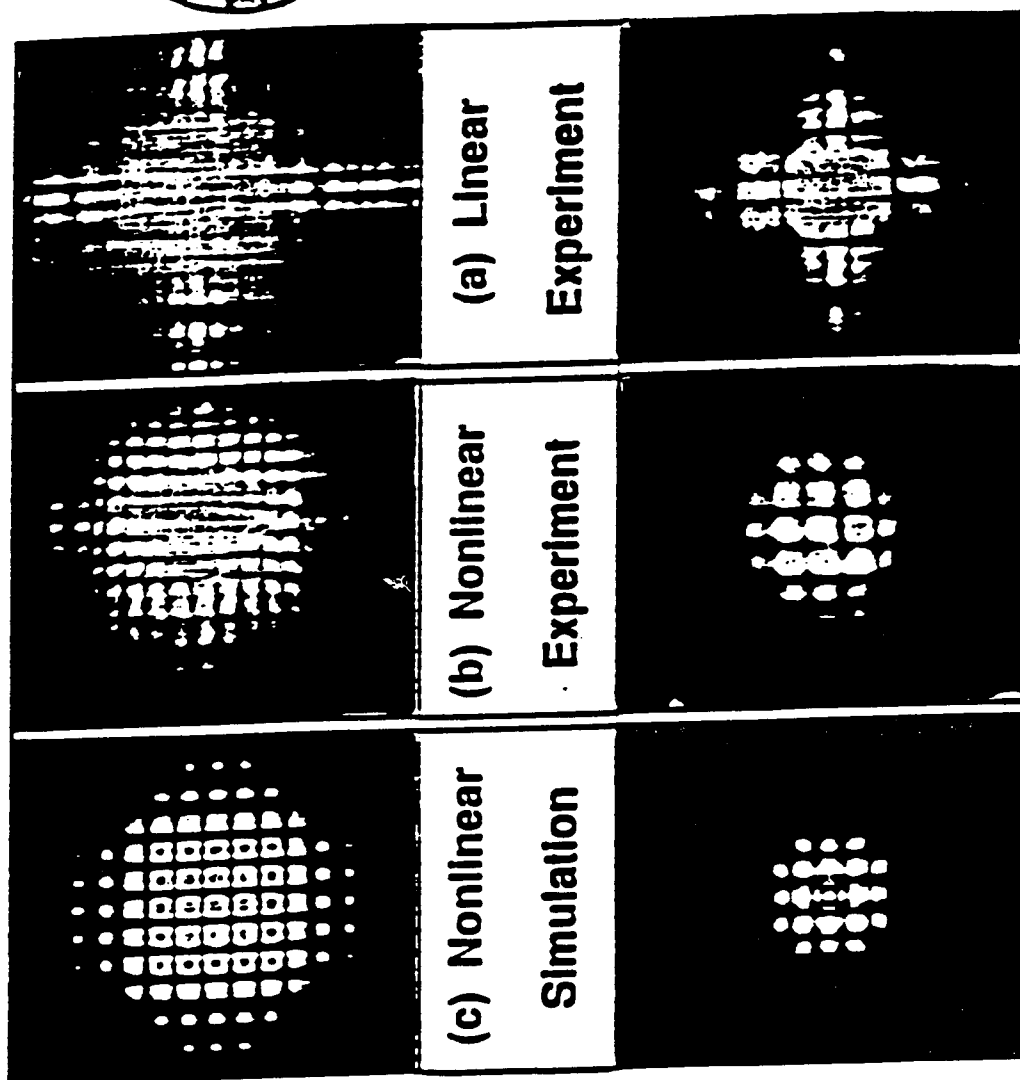
(1) Amplitude (2)
Masks

FIG. 1. Far-field cross-sectional images for propagation through sodium vapor with a wire mesh in the incident plane (column 1) and through an absorbing liquid with the "cross" configuration (column 2).

nonlinear filtering.

Our exploration into SDS's formation was motivated by the observation of intriguing non-linear transformations of far-field (Fraunhofer) diffraction patterns of a wire mesh placed at the input face of a sodium vapor cell (see Fig. 1(1a)). (Far-field diffraction is highly sensitive to intensity-dependent phase changes in a nonlinear layer.) In all the cases studied so far with rectilinear diffraction screens, the linear Fraunhofer diffraction pattern evolves into various arrays of square spots as the laser intensity increases. Subsequent measurements at the output face of the nonlinear medium (in the Fresnel or "near-field" regime) revealed the formation of very distinct dark stripes which had caused those novel nonlinear far-field patterns.

Here we will briefly describe our earlier results and then reflect in more details more recent results, mostly on propagation of dark solitons inside the nonlinear material (near-field patterns), which also included not only "amplitude" masks (i. e. wire mesh), but also "phase" masks (phase step) that enabled us to excite most fundamental single stripe and cross dark solitons. In our initial experiment, a cw frequency stabilized dye laser beam was passed through a wire mesh and then imaged into an $L=18\,mm$ long cell containing sodium vapor, a strongly nonlinear material. The laser frequency was tuned slightly below the D_2 atomic resonance, corresponding to a negative nonlinearity ($n_2 < 0$). The Gaussian beam was dissected first into a ~ 3×3 array of spots (see Fig. 1 (1)). The spectacular transformations of the far-field patterns described above were observed when the laser was scanned from an off-resonance frequency below the D_2 transition frequency, toward the resonance (thereby varying the value of n_2). Fraunhofer diffraction was observed (see Fig. 1(1,a) far off-resonance, where $n_2 \approx 0$. However, as the laser frequency approached the D_2 line (from below), the far-field profile transformed itself into an amazingly well-organized square array of spots, filling the central area of the beam, Fig. 1(1,b). (At the self-focusing side of the D_2 line, where $n_2 > 0$, the transformation was considerably different than that described above and consistent with the earlier results for self-focusing materials.)

The geometric beauty of the far-field patterns and their stability over a relatively large range of intensities and driving field frequencies led us to believe that this phenomenon is not attributed to the specific physics of the nonlinearity in sodium vapor, but rather to the simple fact that the nonlinear component of refractive index is negative, i. e. $n_2 < 0$. To verify this, we tried an experiment using another phenomenon resulting in large values of $n_2 < 0$: the so-called thermal nonlinearity, which can readily be induced using low power radiation in many slightly absorptive liquids. The results of these experiments showed nonlinear far-field patterns amazingly similar to each other and to those of the sodium vapor experiment. Although the nonlinearity due to the thermal effect exhibits some spatial nonlocality, this has not appreciably affected the observed phenomenon, presumably because the characteristic scale of the nonlocality was smaller than the soliton size.

The simplest and probably most fundamental wire mesh configuration is a single opaque "cross" (see Fig. 1(2)). In this case the Fraunhofer pattern (Fig. 1(2,a)) experiences a nonlinear

FIG. 3 Experimental (crosses) and theoretical values (solid line) of the soliton parameter λ_{nl} as a function of the normalized wire width A when the boundary condition is a wire that bisects a Gaussian beam. Inset: Corresponding numerical solution of the (2+1)-D NSE, showing intensity profiles in the plane, $y=0$, and a pair of diverging dark solitons.
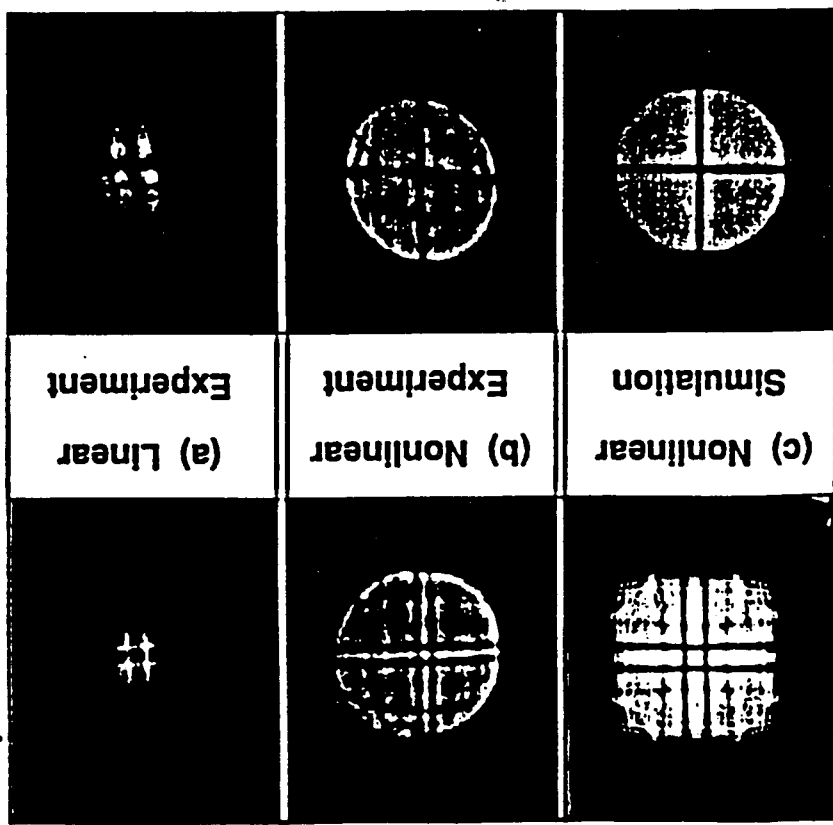

FIG. 2 Near-field cross-sectional images of the output sample face for propagation through an absorbing liquid with an amplitude cross (column 1) and a phase cross (column 2) in the incident plane.
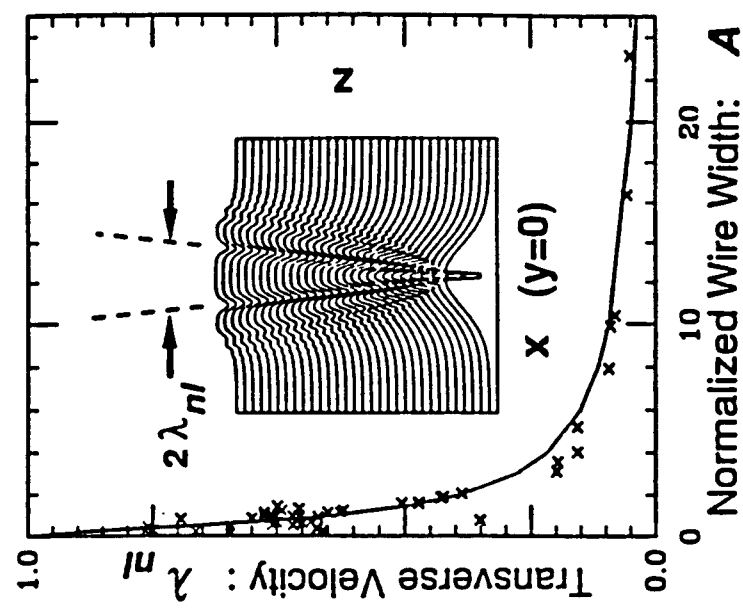
transformation into a grid pattern (Fig. 1(2,b)) that has essentially the same characteristics as the 3 × 3 mesh case (except that there are fewer spots), indicating similar nonlinear transformations in both cases. To understand the observed phenomenon, we modeled the experiment using the (2+1)-D NSE for laser beam propagation in a nonlinear medium:

$$2ik\ \partial E/\partial z\ +\ \nabla_{\perp}^2 E\ +\ k^2 n_2 \left| E \right|^2 E/n_0 = 0 \qquad (1)$$

where $\nabla_{\perp}^2 = \partial^2/\partial x^2 + \partial^2/\partial y^2$ $(=\partial^2/\partial x^2$ for the (1+1)-D NSE), x and y are the transverse coordinates, z is the propagation coordinate, E is the complex electric field, and k is the wavevector in the material. Eq. (1) was solved by us using numerical methods. The simulated far-field results (see Fig. 1(c)) show the same features as the experimental far-field patterns in Fig. 1 (b). The agreement between the experimental and numerical results is remarkable.

In our later research [1,4,24], to identify the physical phenomenon which gave rise to the observed *far−field* patterns, we studied the specific features of wave propagation *inside* the nonlinear material. This was accomplished by examining the *near−field* patterns at the output face of the nonlinear material for different lengths of the material, and for various boundary conditions, including a single wire, two parallel wires, two orthogonal sets of parallel wires, a wire mesh, a single phase jump, multiple phase jumps intersecting at a point, and two parallel phase jumps. The formation of pronounced dark stripes or grids was a universal phenomenon for all the cases studied. In general, the width of each stripe remained almost constant as the thickness of the nonlinear material increased, but decreased as the laser field strength increased. The number of these dark stripes, which tend to appear in pairs, also remained *constant* with propagation distance, even after collisions. These observations, together with the fact that $n_2 < 0$ suggest that the dark stripes are *spatial dark solitons*. Our investigation also shows that, notwithstanding orthogonal interactions, (2+1)-D dark soliton stripes behave amazingly similar to the analytical (1+1)-D dark solitons, i. e., it appears that soliton stripes orthogonal to each other in a cross-sectional plane, propagate almost independently of each other.

To verify that the observed phenomenon was indeed attributed to (2+1)-D dark solitons, we investigated the two most fundamental cases: (*i*) an opaque cross ("amplitude mask", AM) composed of two orthogonal wires, and (*ii*) crossed phase steps ("phase mask", PM) constructed with two microscope cover slips (see Fig. 2 (1) and (2)). The corresponding near-field images are shown in Fig. 2 for a thermal nonlinear material. In the AM case, the linear Fresnel diffraction pattern (Fig. 2(1,a)) exhibits a gray shadow of the cross flanked by bright stripes. In contrast, the shadow is completely missing in the experimental nonlinear profile (Fig. 2(b)); instead, two high contrast dark stripes separated by a distinct bright region, are formed parallel to both axes of the cross. In spite of the magnification in size with increasing beam power due to self-defocusing, the width of the dark stripes actually decreases, as expected for dark solitons.

In the PM case, the linear Fresnel diffraction pattern displays a broad dark cross aligned with the axes of the phase steps, flanked by diffractive ringing. As the laser power is increased

(see Fig. 2(2,b)), the width of the central cross decreases (even at the intersection) and does not split into two (as did the shadow of the dark opaque cross in Fig. 2(b)). This also occurs in a (1+1)-D nonlinear system when the boundary condition is a π phase step, with the central dark stripe referred to as a "fundamental dark soliton"; similarly, the pattern in Fig. 2(2b) can be regarded as a "fundamental dark soliton cross." Our numerical solutions for both nonlinear cases, shown in Fig. 2(c), again reaffirm that Eq. (1) correctly predicts the observed phenomena.

A strong verification of the soliton nature of the the observed phenomenon was achieved by comparing [1] experimentally measured parameters with the theory. We measured the soliton divergence angle, θ, with respect to the optical axis (see inset of Fig. 3), to determine the soliton characteristic parameter, $\lambda_{nl} = \theta \eta_{nl}^{-1/2}$ (the soliton amplitude and width also depend on λ_{nl}), where $\eta_{nl} \equiv |n_2| \, |E|^2/2n_0$. When a single wire of diameter, x_A, is small compared to the beam size, then λ_{nl} is determined by the equation $\lambda_{nl} \approx \cos(\lambda_{nl}kA)$, where $A = x_A \eta_{nl}^{1/2}$. The excellent agreement between the data and theory is shown in Fig. 3. The inset (Fig. 3) illustrates the formation of a pair of diverging dark solitons for the case of a single wire. To test the integrity of dark solitons on a *finite* (e. g., Gaussian) background, we computed the so-called "soliton constant" , and found that this parameter was nearly constant ($=1.76^2/n_0 n_2 k_0^2$). This indicated that these dark stripes propagate as robust formations, even though the background intensity relaxes adiabatically due to self-defocusing and linear diffraction.

The *far$-$field* transformation of a linear Fraunhofer pattern into a tightly organized and ordered nonlinear pattern (as in Fig. 1) can now be explained, in terms of the formation of spatial dark soliton stripes and grids. This effect occurs, in general, because some spatial-frequency components of the incident beam are channeled into the formation of solitons, and thus are not allowed to "radiate" away from the optical axis as in the linear case.

In conclusion, we have observed the nonlinear transformation of various Fresnel and Fraunhofer diffraction patterns of a laser beam passing through a rectilinear amplitude or phase mask, followed by a self-defocusing material. Under nonlinear propagation, spatial dark solitons formed, appearing as dark stripes or grids in the beam cross-section. The (2+1)-D soliton structures behaved as if they consisted of two almost independent and noninteracting (1+1)-D soliton substructures. The similarity between our experimental data and numerical solutions of the (2+1)-D NSE was remarkable.

2.iii. Amplification, Instability, and Chaos in Nonlinear
Counterpropagating Waves

In the pilot paper under previous AFOSR support and mostly in the extensive exploration effort under this grant [3,5,22,32,40], this principal investigator and Dr. Chiu Law demonstrated for the first time that two linearly polarized counterpropagating waves in a Kerr nonlinear medium with linear dispersion can exhibit amplification and multi-mode temporal instability,

which are attributed to the combined effect of nonlinear index grating and linear dispersion. We also explored possible use of this effect for large broad-band amplification that may exist in the system (in particular in a nonlinear optical fiber) if the pumping is below the threshold of instability. This amplification can have a significant potential for such applications as optical fiber communication.

The cross-interaction of two counterpropagating laser beams in a third order nonlinear material is a conceptionally simple and fundamental process in nonlinear optics. In the research done under this grant, it has been shown [3,5,22] that regular linear dispersion (i. e. frequency dependence of refractive index) can be a natural and universal agent for amplification of perturbations and temporal instability in the counterpropagating nonlinear waves. It is well known that linear dispersion can give rise to nonlinear optical effects such as spatial instability of single plane wave, formation of soliton in nonlinear fiber, and amplification of counterpropagating waves. This suggests that linear dispersion in combination with non-linear processes can dramatically change the dynamical behavior of a system.

In our pilot research we started investigation of stability of eigenpolarization. The total complex electric field of the two counterpropagating plane waves in the Kerr nonlinear medium was represented as: $\vec{E} = [E_1(z,t)e^{ikz} + E_2(z,t)e^{-ikz}] e^{-i\omega t}\hat{e}_x$ where $E_1(z,t)$ and $E_2(z,t)$ are the slowly varying envelopes of forward (+z) and backward (-z) propagating waves respectively. The dynamics of these envelopes is governed by two coupled nonlinear Schrodinger equations:

$$i\left[(-1)^{j+1}\frac{\partial E_j}{\partial z} + \frac{1}{v_g}\frac{\partial E_j}{\partial t}\right] - \frac{\mu}{2}\frac{\partial^2 E_j}{\partial t^2} = -\beta(2I_{3-j} + I_j)E_j ; \quad j = 1, 2 \tag{1}$$

where $I_j = |E_j|^2$ is the intensity of the respective propagating wave, $\mu = \partial^2 k/\partial\omega^2$ is the linear dispersion parameter, $\beta = n_2 k/n$ is the nonlinear parameter, n is the linear refractive index at the frequency ω, v_g is the linear group velocity, n_2 is the nonlinear refractive index coefficient, and k is the wave number in the medium. The coefficient 2 in the right-hand side in Eq. (1) reflects light-induced nonreciprocity.

To analyze the small perturbation stability of the steady state and also the amplification, we represented both waves in the system as slightly perturbed steady state in the form:

$$E_j = E_{j0}(\xi)[1 + A_{1,j}(\xi)e^{\lambda\tau} + A_{2,j}^*(\xi)e^{\lambda^*\tau}] \tag{2}$$

where $j=1,2$, E_{j0} is the steady solution for Eq. (1), $A_{1,j}$ and $A_{2,j}$ are normalized amplitude of the small perturbations, $\tau = tv_g/L$ is the normalized time, and $\xi = z/L$ is the normalized distance of propagation, with L being the total length of nonlinear material. Substituting Eq. (2) into Eq. (1) and linearizing the latter equation, we obtained [3,5,22] linear propagation equations for $A_{k,j}$ and solved them. We assumed for simplicity equal intensities of the waves, i. e. $I_{10} = I_{20} = I$. Using the boundary conditions for the perturbation amplitudes we obtained [3,5,22] an equation

for λ and solved it.

The details of our results can be found in [3,5,22]; some preliminary new results have been reported by us previously. We will briefly summarize our results on instabilities and will give a bit more details on the most recent results on amplification (especially in fiber waveguides pumped by the counterpropagating waves). We found the boundaries of instability in the space of parameters of the system (dispersion, nonlinearity, pumping intensity and the length of the nonlinear system). For further discussion we introduce dimensionless parameters: $p = \beta IL$ -- normalized pumping intensity (note that p can have negative sign depending on non-linearity β), and $d = \mu v_g^2/(2L)$ -- normalized dispersion. We found that the entire domain of instability consists of multitude of individual unstable modes, and we found solutions for them. These individual modes essentially are longitudinal modes in a light-induced, distributed-feedback resonator. We found also the boundary encompassing all the unstable solutions. The (encompassing) threshold intensity increases as dispersion decreases; our numerical calculations show that for sufficiently small $|d|$, this dependence can be best described by a surprisingly simple relationship

$$p_{cr} = -sgn(pd)\,|\log_\eta |d|\,| \tag{3}$$

where η is numerically determined to be 10.0±1%, and sgn(pd) is the sign of pd. The necessary condition for initiating instability (i. e. to have $p_{cr} > 0$) is that the signs of nonlinearity n_2 and dispersion μ must be opposite, which coincides with the necessary condition for formation of a soliton and spatial instability in single-wave propagation.

When the pumping is only slightly above the threshold, only one mode become unstable, then two, and so on. When the number of modes is greater than one, they compete with each other and some of them can become dominant while others fade out. If only one mode is unstable, it eventually develops into periodic self-sustained oscillations with a stable amplitude. When the value of $|p/p_{cr}|$ is increased above 1.28, the instability and resulting self-sustained oscillations develop much faster; as the oscillations develop in time, the second subharmonic is excited which later evolves into aperiodic oscillations with randomly modulated amplitude and phase indicating onset of chaos. This behavior further develops into strongly pronounced chaos when the pumping intensity is significantly exceeds the threshold of instability, Eq. (3).

To estimate the threshold intensity for instability, consider an example of a 1 km long single-mode fiber with Ge-doped silica core at wavelength 1.55 μm with group velocity dispersion D(k) = 6.5×10^{-3} [note that $\mu = -D(k)/(kc^2)$] (the corresponding $d = -8.02\times10^{-13}$), refractive index n = 1.44, and $n_2 = 3.2\times10^{-16}$ cm^2/W , in the lossless approximation. We find the threshold intensity I_{cr}, Eq. (4), for such a fiber to be 10^7 W/cm^2, which is below the damage threshold 10^{10} W/cm^2 for fused silica. Crude estimate shows that the losses existing in the real fiber ($\sim$0.5 dB/km) would require only about two times higher threshold intensity. If we use the SF-59 glass with $n_2 = 7\times10^{-15}$ cm^2/W at wavelength 1.06 μm, and assume that n_2 at wavelength 1.55 μm is of the same order as that of 1.06 μm and that dispersion is roughly the same as for plain glass, the critical intensity is reduced to $\sim$425 kW/cm^2 for the same length.
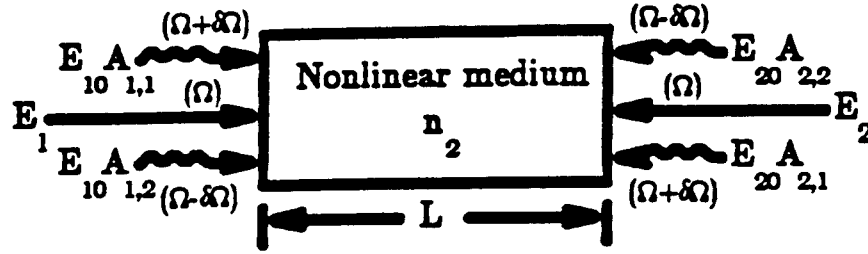
Figure 4. Pump-probe configuration for amplification measurement where E_1 and E_2 are pumping waves and $E_{10}A_{1,1}$ is the input probe wave with $E_{10}A_{2,1}$, $E_{20}A_{1,2}$ and $E_{20}A_{2,2}$ generated as a result of the wave mixing process.
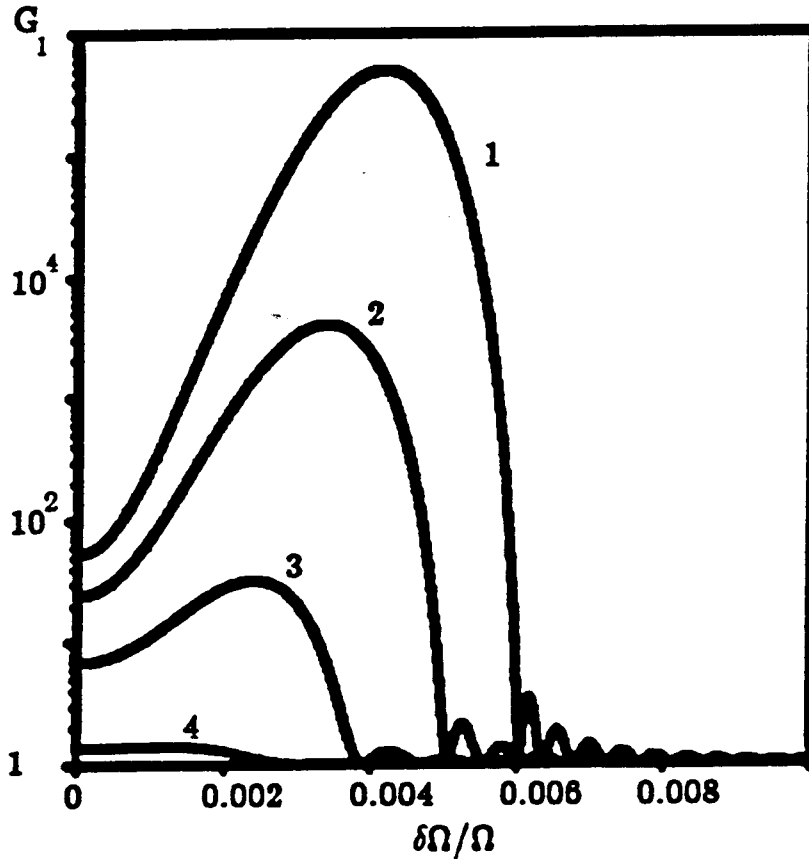

Figure 5. Amplification G_1 of the probe wave versus frequency modulation index $\delta\Omega/\Omega$ for the case of a 1 km long Ge-doped silica fiber. (Curves: 1 — 60% of instability threshold p_{cr} [120 times of the amplification threshold, I_{amp}], 2 — 40% of p_{cr} [80× of I_{amp}], 3 — 20% of p_{cr} [40 × of I_{amp}], and 4 — 5% of p_{cr} [10 × of I_{amp}]).

The most interesting opportunity provided by systems in consideration, is amplification of a weak probe signal under counterpropagating pumping, when the pumping is way below the instability threshold. To find the gain spectrum of this system, we inject a weak probe beam into the nonlinear medium and scan the beam frequency. In Fig. 4, we show a configuration with two pump beams and four weak beams. Suppose that the probe beam $(E_{10}A_{1,1})$ has frequency of $\Omega + \delta\Omega$, i. e. its frequency deviated from that of the pump beams with normalized frequency Ω by $+\delta\Omega$; then we expect a phase conjugate signal $(E_{20}A_{2,2})$ to be reflected back with frequency $\Omega - \delta\Omega$.

Our numerical results are shown in Fig. 5. We define the intensity amplification G_1 for the probe wave $A_{1,1}$, as: $G_1 = |A_{1,1}(\xi=1)/A_{1,1}(\xi=0)|^2$. The variation of G_1 versus normalized frequency detuning $\delta\Omega$ is depicted in Figs. 5 for the 1 km long Ge-doped silica fiber with pumping at 60%, 40%, 20%, and 5% of the threshold intensity $I_{cr} = 9.3 MW/cm^2$. One can see that even when the pumping is well below the threshold of instability, the bandwidth and amplification are still appreciable. For instance, in the case of pumping at 20% of the threshold of instability the gain ≈ 20 and bandwidth $\approx 2.5 \times 10^6$ (7.4×10^{11} Hz or 0.4% of the pumping frequency).

Under realistic conditions $d \ll 1$, we found a good analytical approximation for the gain G_1 [3,5,22]. We shoved that the gain spectrum differs significantly between detuning domains separated by the detuning $(\delta\Omega)_o = (8|pd|)^{-1/2} \ln(1+p^2)$. The portion of the gain spectrum for $\delta\Omega \ll (\delta\Omega)_o$ corresponds to the contribution from dispersionless four wave mixing. Beyond $(\delta\Omega)_o$, the variation of gain obeys $\sim \exp(2\delta\Omega[2|dp| - (d\delta\Omega)^2]^{1/2})$ when pumping power $|p|$ is substantially below p_{cr}. This part of the gain is solely caused by dispersion-related process.

We found that a nonzero amplification (or $G_1 > 0$) can be obtained for any pumping intensity, however, for each fixed intensity $|p|$, the frequency detuning should be smaller than certain cutoff frequency, $(\delta\Omega)_{cr}$,

$$|\delta\Omega| \leq (\delta\Omega)_{cr} \approx \sqrt{2|p/d|} \ .$$

Therefore, a rough estimate of the amplification bandwidth is given by $(\delta\Omega)_{cr}$, Eq. (4), which is valid for arbitrary pumping, $|p| < p_{cr}$. The maximum bandwidth $(\delta\Omega)_{max}$ for a fixed dispersion d is attained when $|p| = p_{cr}$, Eq. (3), i. e.

$$(\delta\Omega)_{max} \approx \sqrt{2|\log_\eta |d||/d|} \ .$$

The location of the peak gain $(\delta\Omega)_{opt}$, i. e. the frequency of the mode with lowest threshold of instability, can be approximately estimated as:

$$(\delta\Omega)_{opt} = (\delta\Omega)_{cr}/\sqrt{2}$$

The results are qualitatively close to the exact values from numerical calculation shown in Fig. 5. All of them indicate that the nonlinear fiber with dispersion, pumped by counterpropagating waves has great potential as an all-optical amplifier operating in cw or quasi-cw regime which may find application in optical gyroscopes, optical fiber communications, etc. One possible

limiting factor in amplification is the losses in the fiber which have not been included in our calculation. To estimate the effect of losses in the optical fiber, we introduce a threshold intensity of amplification I_{amp}, which satisfies the condition: $\alpha L = \Gamma(I_{amp})$, where α is the loss coefficient and $\Gamma(I_{amp}) = \ln[G_1(I_{amp})]$ is the growth rate at the amplification threshold in the lossless approximation, i. e. the gain must be equal to loss at I_{amp}. We obtained [3,5,22] a remarkably simple expression for I_{amp} at $(\delta\Omega)_{opt}$:

$$I_{amp} = \alpha/(2n_2 k) \tag{4}$$

which does not depend on either length or dispersion. For the silica fiber with $\alpha = 0.5 dB/km = 0.12\,km^{-1}$ and $n_2 k = 1.3 \times 10^{-6}\,km^{-1}$. Hence, the threshold of amplification is $46.2 kW/cm^2$ (or 0.5% of the threshold of instability in the example with $L = 1km$ and $\mu = 14\,psec/nm - km$). For a typical fiber with effective area of 50 μm^2 , the threshold pumping power for amplification is 23mW. This excellent projected performance is due to the low loss in the fiber.

To conclude this section, we discovered that linear frequency dispersion together with Kerr nonlinearity can result in amplification and temporal instability of nonlinear counterpropagating waves. As the pumping increases above certain threshold, self-oscillations are excited; upon further increase of pumping they evolve into subharmonics and chaos. With under-threshold pumping, large gain and broad-band amplification are to be found. The mechanism of the entire phenomenon can be explained in terms of positive distributed feedback from the nonlinear index grating formed by the two laser beams. Our calculations show that the amplifiers based on the nonlinear optical fiber pumped by counterpropagating waves with relatively low power have great potential for various applications.

2.iv. Field-Gradient-Induced Second Harmonic Generation in Vacuum

In this research we revised our previous result on QED-based SHG in vacuum. Our new results [11,15,20] show that the photon-photon scattering in vacuum can give rise to the second-harmonic generation of intense laser radiation in a dc magnetic field (even in the "box" diagram approximation of quantum electrodynamics which was a source of some controversy in the literature) if the symmetry of interaction is broken by *nonuniformity* of optical wave + dc field system in time or/and space. Specific examples considered by us were: optical *pulse* plane wave and a *Gaussian* laser beam propagating in either uniform or nonuniform dc field.

Photon-photon scattering (PPS) is perhaps one of the most fundamental quantum electrodynamics (QED) processes which may also result in nonlinear optical effects in vacuum such as the birefringence of the refractive index seen by a probe field under the action of either a dc magnetic (or electric) field, or intense laser pumping, multiwave mixing, and merging of two photons into one (i. e. sum frequency generation) under the action of a dc field. If observed, these effects may provide a fundamental optical test of QED. All of these effects are based on the lowest order, so called "box" diagram approximation. Yet the required optical fields are still

enormously high and not presently available. It has also been apparent that a dc field (either electric or magnetic) may greatly assist the interaction. However, perhaps the most interesting dc field-assisted processes: the merging of two photons into one (e. g. the second harmonic generation, SHG) and photon "splitting" (in essence, a parametric process) in the presence of a dc field -- have caused a long standing controversy (see review in [15,16]), with the results on the probability of the photon splitting and merging differing by many orders of magnitude. Most recently, we have proposed (in the work under the earlier AFOSR grant, Y. J. Ding and A. E. Kaplan, Phys. Rev. Lett. 63: 2725 (1989)) the SHG of laser radiation in vacuum in the presence of a dc magnetic field. As result of the discussion (Phys. Rev. Lett. 65, 2744-2746 (1990)) following that publication, we came to the conclusion [11,b] that the result for box diagram vanishes for a *cw plane* wave and an *uniform* dc field which was essentially the main case considered earlier; we also suggested that the nonvanishing effect may result from the *nonuniformity* of dc field.

Thus, aside from the issue of immediate observability, the fundamental question arises whether the vanishing contribution of the box diagram is due to some fundamental laws of QED, or only to the chosen configuration: plane monochromatic (cw) optical wave + uniform dc field. In our most recent research [11,15], we showed that the nonvanishing contribution of the box diagram can result from the nonuniformity (or gradient) of *any* component of the *entire* field system (in particular - optical field) in *space* or/and *time*. In particular, we considered (i) plane wave modulated in time by a pulse with an arbitrary profile and finite duration, and (ii) a cw Gaussian beam in magnetic field with an arbitrary spatial distribution, and show that in these configurations nonvanishing SHG in the lowest (i. e. box) approximation can result from the laser beam propagating either in a uniform or nonuniform dc fields. The total number of SHG photons in such a system is $\sim 10^{16} - 10^{24}$ orders of magnitude higher than that due to the next, hexagonal diagram contribution [11,15], such that SHG appears to be truly of the "box diagram" nature.

The Heisenberg-Euler Lagrangian for PPS can be expanded as $L = L_0 + L_4 + L_6 + \cdots$, where $L_0 = (E^2 - B^2)/2$ is a linear term, and $L_4 = (\xi/2)[(E^2 - B^2)^2 + 7(\vec{E} \cdot \vec{B})^2]$ -- first nonlinear term that corresponds to the box Feynman diagram. Here $\xi = \alpha/45\pi B_{cr}^2 = 2.6 \times 10^{-32} Gauss^{-2}$ is a nonlinear interaction constant with $\alpha = e^2/\hbar c = 1/137$ being the fine structure constant and $B_{cr} \equiv m_0^2 c^3/e\hbar = 4.4 \times 10^{13} Gauss$ -- the QED critical field. L_6 corresponds to the hexagonal Feynman diagram, etc. Following standard procedures one obtains the macroscopic equations in the form of classical Maxwell's equations: $\nabla \cdot \vec{B} = 0$, $\nabla \cdot \vec{D} = 0$, and $\nabla \times \vec{E} + (1/c)\, \partial \vec{B}/\partial t = 0$ $\nabla \times \vec{H} - (1/c)\, \partial \vec{D}/\partial t = 0$, with the constitutive relations between the electric displacement $\vec{D}$ and magnetic field $\vec{H}$, and electric field $\vec{E}$ and magnetic induction $\vec{B}$ in the form $\vec{D} = \vec{E} + \vec{D}^{NL}$ and $\vec{H} = \vec{B} + \vec{H}^{NL}$, where

$$\vec{D}^{NL} = \partial L_4/\partial \vec{E} = \xi(2a\vec{E} + 7b\vec{B}), \qquad \vec{H}^{NL} = -\partial L_4/\partial \vec{B} = \xi(2a\vec{B} - 7b\vec{E}), \tag{1}$$

with $a = E^2 - B^2$ and $b = \vec{E} \cdot \vec{B}$. A cw plane wave does not exhibit any nonlinear effects, since due to its properties, $E^2 = B^2$, $\vec{E} \cdot \vec{B} = 0$, the nonlinearity, Eq. (1), vanishes. This "degeneracy"

of the *third—order* nonlinearity can be broken by the field nonuniformity that can give rise to *second—order* nonlinear *optical* effects in the presence of a strong *static* field.

In our most recent work we considered both spatial [11,a], [15] and temporal nonuniformity [15]. The perhaps simplest and fundamental example of temporally nonuniform wave is *a pulse plane wave propagating in a uniform dc magnetic field* normal (say along the axis y) to the wave propagation axis ($\vec{B}_{dc} = B_0 \hat{e}_z$). Suppose that the amplitude (and/or phase) of fundamental plane wave is *arbitrarily* modulated in time with a (complex) envelope $u_1(\psi)$, where $\psi = \omega_1 t - \vec{r} \cdot \vec{k}_1$ is a "retarded time", and polarized parallel to the dc magnetic field (this polarization provides maximum effect). The plane wave solution for the SHG amplitude, u_2, is found then as

$$\vec{u}_2(\psi, y) = -7(\xi/2) k_1 B_0 \hat{e}_x \{d[u_1^2(\psi)]/d\psi\} \cdot y, \qquad (2)$$

assuming that the field B_0 is "turned on" at $y = 0$. Eq. (2) demonstrates the same dependence on the *distance* of interaction ($u_2 \propto y$) as for SHG in a "classical" nonlinear medium with ideal phase-matching, with the significant difference being that SHG is proportional now to the *time—derivative* of the driving envelope. The use of very *broad spectrum* radiation can further enhance the SHG effect.

We also considered *spatial* nonuniformity [11, 15] of nonplanar (in particular, Gaussian) wave; we assumed a *cw* wave (it is clear, however, that a combined time/space nonuniformity may significantly enhance the nonlinear interaction). We found that predominant contribution to SHG is due to the transverse component of dc magnetic field. Briefly, our results can be summarized as following. In the case when the fundamental wave is a linearly polarized Gaussian beam (*TEM*$_{00}$ mode), we found that a "forced" analytical solution for vacuum SHG consists of *two* modes: one of them, the SHG *main* mode, is similar to the fundamental (laser) Gaussian beam, while another one is a higher order, so called "doughnut" Gaussian mode, with zero amplitude at the center of the SHG beam.

If the *dc* magnetic field is *symmetric* with respect to the position of the beam waist ($y=0$) and extends at the distance much greater than diffractional distance, we showed that the *main* SHG Gaussian component vanishes in the far field area, which is consistent with the conventional nonlinear optics. Thus, this SHG component could be regarded as an analog of "classical" SHG process whereas the doughnut component is a feature peculiar only for gradient nonlinearity.

We considered a few specific cases, in particular *uniform* and *nonuniform* dc magnetic fields. In the case of *uniform* dc magnetic fields, we showed that in most of the cases of interest, the doughnut component contribution exceeds that of the main Gaussian component by order of magnitude or more. For the arrangement whereby the waist of the laser beam is located exactly in the center of the *dc* magnetic field, the main component contribution at the exit point vanishes completely. In this case, the number of SHG photons peaks at the waist of the beam; however, at the exit point the SHG output decreases and tends to some constant,

which is due to the only surviving doughnut component. For the fixed length of interaction, the number of SH photons is maximal, when the waist of the beam is positioned at either the output or input point, We also considered a *nonuniform dc magnetic field in the form of a magnetic dipole*, originated by two thin parallel "magnetic" wires positioned in the plane orthogonal to the laser beam. We showed that in such a case, the SHG out can be significantly enhanced.

An interpretation of nonvanishing SHG in the nonuniform fields is that the nonuniformity allows for momentum transfer between photons and dc field (which would ultimately result in the recoil of material system generating the dc field), thus breaking the symmetry that causes vanishing interaction of completely uniform field system. This explanation could be directly corroborated e. g. by direct QED calculations of SHG by two collinear photons + elementary source (particle) of dc field, similarly to quasi-elastic scattering of *single* photon at a Coulomb potential. Examples of such sources could be protons (or heavy nuclei) or neutrons with two collinear photons "SHG-scattered" at the particle spin and Coulomb dc (electric) field. In macroscopic terms, the SHG is originated by an elementary multipole source, in a limited spatial volume $\ll \lambda_1^3$; we found that in the lowest approximation, the source is a dipole for a spin and a quadrupole for a Coulomb field.

Thus, we demonstrated the feasibility of field-gradient-induced SHG by the intense laser radiation in a dc magnetic field in vacuum; the effect does not vanish in the QED box diagram approximation only if the participating fields are temporarily/spatially nonuniform.

2.v. Nonlinear Optical Research on Semiconductor Films and Quantum Well Structures.

Part of the effort of this PI is devoted to experimental research on nonlinear optics of semiconductor, in particular thin ZnSe films and superlattices and quantum well of various compositions. To the extend, this is a continuation of pioneering studies on nonlinear properties of ZnSe attributed to resonant excitons. Another reason for this interest was to use self-bending effect (first predicted by this PI in 1969) for the first time for nonlinear spectroscopy of nonlinear refractive index, in particular in ZnSe (see Section 2.v.1 below). This research was a collaborative effort between research groups of this PI and Dr. J. Khurgin at the same department. The main thrust of the *rest* of research on nonlinear optics of semiconductors was concentrated on asymmetric quantum wells which is mostly in the area of research interests of Dr. J. Khurgin and his group; it will be addressed here only very briefly (see Section 2.v.2 below).

2.v.1. Spectral Measurement of Nonlinear Refractive Index in ZnSe
Using Self-Bending of a Pulsed Laser Beam

In this research [2,21], this PI's research group (including Y. J. Ding, G. Swartzlander, and C. T. Law) collaborated with Dr. J. B. Khurgin's research group on first *spectral* measurements of nonlinear refractive in ZnSe using self-bending of a pulsed laser beam. The effect of self-bending has been predicted by this PI in 1969 and subsequently observed experimentally in pulse regime in NaCl crystal, and recently in CS_2; the first observation and measurements in cw regime (using sodium vapor as a nonlinear medium) has been done by G. Swartzlander (then a grad student) and this PI under AFOSR support. One of the natural applications of that effect was to use it for direct measurements of nonlinear refractive index. Our measurements of the nonlinear refractive index (n_2) spectrum of ZnSe near the band gap ($\lambda_{gap} \sim 450\,nm$) at 77 K showed that the maximum nonlinearity, $n_2 \sim 1.9 \times 10^{-8}\,cm^2/W$, measured by us, was anomalously large to be explained by conventional thermally-induced bandgap shrinkage (TIBS).

ZnSe is one of the semiconductor materials with large nonlinear refractive index especially in the blue domain ($\lambda_{gap} \sim 450\,nm$ at 77 K). Although it is believed that this nonlinearity is basically due to TIBS, the nonlinear mechanisms are still not completely understood. The measurements of the spectrum of nonlinear refractive index in the vicinity of resonant transitions (e. g. excitonic or band edge transitions) are crucial for the physics and device applications of these materials. Although many new techniques for these measurements have been proposed, none of them was simple enough to be used for measuring the entire spectra of nonlinear refractive index in semiconductors.

The self-bending method for measuring spectrum $n_2(\lambda)$ has several advantages over other methods. It requires in principle a single shot per data point (λ) (although due to lack of the detection equipment required for that, our measurements here were based on multi-shot averaging), whereas e. g. the Z-scan technique inherently involves many shots and requires high mechanical and laser shot-to-shot in which two (pump and probe) laser beams are required and the results for n_2 are obtained indirectly by using Kramers-Kronig transformation. Finally, the sign of n_2 can be immediately and directly determined from the direction of self-bending effect.

An ideal case of self-bending occurs when a slab beam with a "triangular" spatial intensity profile in the beam cross-section propagates through a Kerr-like nonlinear medium with the refractive index $n \approx n_0 + n_2 I$, where n_0 is the linear refractive index and n_2 the coefficient of nonlinearity. Since a nonlinear prism is induced in the beam path, the beam (in the transparent nonlinear material) will be self-deflected in the far-field region by the angle θ_{NL},

$$\theta_{NL} = n_2 L I_0 / a_0 \tag{1}$$

where a_0 is the beam size, L is the thickness of the nonlinear medium and I_0 is the laser peak
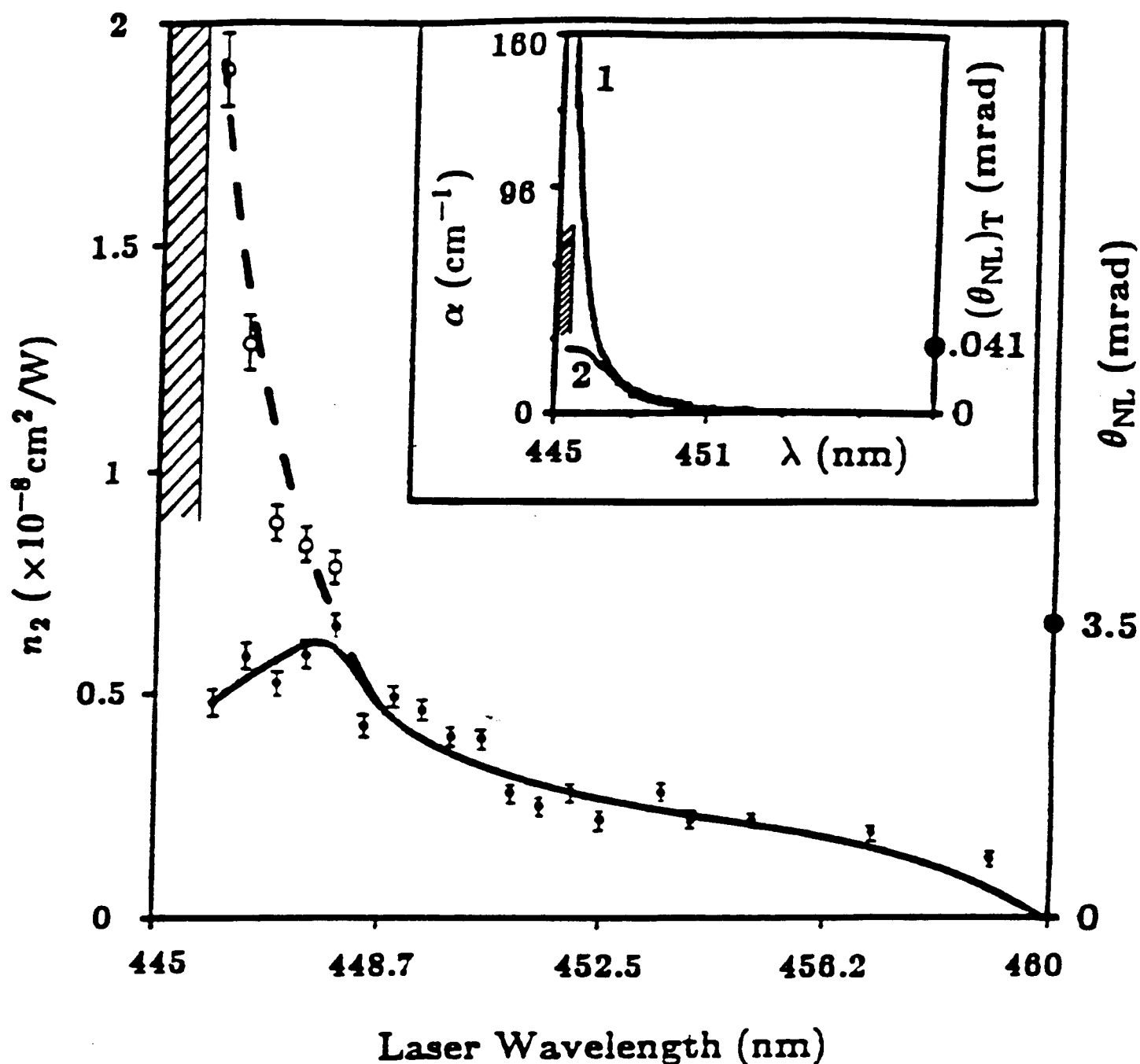
Fig. 6 The measured spectra of self-bending angles θ_{NL} (dots - experimental data, solid curve - the least square fitting) and of nonlinear refractive index n_2 (circles - recalculated experimental data, broken curve - the least square fitting) vs. the laser wavelength. Inset: the measured spectra of absorption (α), curve 1, and of self-bending angle due to TIBS $(\theta_{NL})_T$, curve 2, for $I_0 \sim 1.5 \times 10^5$ W/cm^2. The shaded area corresponds to strong absorption of the laser beam.

intensity penetrating into the nonlinear medium. For our experiment parameters, our calculations show that typical value for the relative error introduced with the use of right-triangular model instead of a semi-Gaussian profile used in experiment was less than 10%. In our experiment, we observed the self-bending effect in bulk ZnSe over the range 446 nm - 460 nm with maximum n_2 as large as $1.9 \times 10^{-8} cm^2/W$.

The details of experimental set-up and the parameters of the laser pulse, lenses, etc., can be found in Refs. [2,21]. Here we will briefly discuss the results of the experiment. The measurement of the spectrum of the self-bending angles for different laser wavelengths is shown in Fig. 6 (the dots and solid curve). For this measurement, the laser peak intensity was $I_0 \sim 1.1 \times 10^5 W/cm^2$ and λ ranged from 446 nm to 460 nm. The self-deflection angle θ_{NL} had a clear maximum at ~448 nm, where $\theta_{NL} \approx 3.5 \ mrad$. The spectrum $n_2(\lambda)$ can be determined using Eq. (1) and measured spectrum of θ_{NL}. However, our measurement of absorption shows that the absorption may become significant near the bandgap (e. g. ~30% at $\lambda \sim 448 \ nm$, see inset in Fig. 6 and text below). Because of that, n_2 should be corrected using Eq. (1) where now the term $L I_0$ is to be replaced by $\int_0^L I(x)dx = I_0 (1 - e^{-\alpha L})/\alpha$, where $\alpha(\lambda)$ is the absorption coefficient at wavelength λ. The absorption spectrum of laser beam in ZnSe was measured at peak laser intensity $I_0 \sim 1.5 \times 10^5 \ W/cm^2$ and is plotted in inset of Fig. 6. Based on this procedure and using original measurements of self-bending angles (solid curve in Fig. 6), we had calculated the spectrum of n_2 which is plotted in Fig. 6 (broken curve). We were unable to measure n_2 for the laser wavelength below ~ 446 nm because of strong band-edge absorption (shaded area in Fig. 6). Our experimental results showed that ZnSe materials demonstrated Kerr-like nonlinearity with no saturation up to the maximum laser peak intensity ~ $3.1 \times 10^5 \ W/cm^2$, measured in the experiment, which was verified by the fact that the self-bending angles were linear in the laser intensity, I_0, see Eq. (1).

The spectrum of nonlinear refractive index obtained by us could be immediately used in attempt to either identify the mechanism of the observed effect or at least rule out some of the known mechanisms. Although there are a few nonlinear mechanisms described in the literature, the commonly believed dominant effect contributing to nonlinear refractive index near the bandgap is TIBS. Assuming the worst case scenario whereby no heat transfer takes place during a single laser pulse, the maximum increase of the local temperature in the sample due to heating with the laser pulse energy penetrating into the nonlinear medium J_{laser} is

$$(\Delta T)_{max.} = (\Delta T)_0 \, e^{-\alpha x} ; \quad (\Delta T)_0 \approx J_{laser} \, \alpha / \pi \, c_p \, a_0^2 \qquad (2)$$

where x is the distance from the entrance interface of the laser beam and $c_p \approx 0.34 \ J/K \cdot cm^3$ is the heat capacity of ZnSe at 80 K. From the absorption spectrum shown in the inset in Fig. 6, one can determine that the maximum absorption coefficient measured over 446 nm - 460 nm is ~74 cm^{-1} at $\lambda \sim 446 \ nm$. In our experiment, with the typical $J_{laser} \sim 2.2 \times 10^{-7} \ Joule$, $a_0 \sim 100 \ \mu m$, and $L \sim 500 \ \mu m$, the absorption can increase the temperature of the sample at the boundary ($x = 0$), Eq. (2), by ($\Delta T)_0 \approx 0.15 \ K$ at $\lambda = 446 \ nm$. Consequently, the band gap

decreases by $\Delta E_g = (dE_g/dT) \cdot \Delta T$, where $dE_g/dT \approx -8 \times 10^{-4}$ eV/K, i. e. $\Delta E_g \sim -1.2 \times 10^{-4}$ eV. Using Moss rule we determine the contribution to the spectrum of nonlinear refractive index due to TIBS as $\Delta n = (-dE_g/dT) n_0 \Delta T /4E_g$. Using now Eq. (2), it can be translated into the self-bending angle due to TIBS as

$$(\theta_{NL})_T = J_{laser} \, n_0 \, (-dE_g/dT) \, (1 - e^{-\alpha(\lambda)L})/4\pi E_g \, c_p \, a_0^3 \qquad (3)$$

where the linear dispersion of refractive index is negligible here. Spectrum of $(\theta_{NL})_T$ calculated from Eq. (3) where $n_0 \approx 2.8$, is plotted in the inset in Fig. 6. The peak θ_{NL} measured by us in Fig. 6 occurs at $\lambda \sim 448\,nm$ and θ_{NL} reaches 3.5 mrad. At the same wavelength, the self-bending angle calculated based on TIBS is only $(\theta_{NL})_T \sim 1.3 \times 10^{-5}$ rad, i. e. at least two orders of magnitude smaller. In order to further verify that the spectrum of the self-bending angle measured by us was not due to TIBS, it is instructive to also compare the shapes of the spectra of both mechanisms. This comparison shows that whereas the spectrum for TIBS plateaus in the vicinity of fundamental bandgap (see inset in Fig. 6), our measured spectrum has a distinct maximum. TIBS due to repetitive laser pulses can also be ruled out since far-field intensity profile was independent of repetition rate (1 Hz - 10 Hz). Thus, we can rule out TIBS as a mechanism of the observed nonlinearity. Saturation (band filling) and free-carrier effects can also be ruled out since they both result in negative n_2. Further investigation is apparently required to determine the real nature of the observed nonlinearity.

In conclusion, the nonlinear refractive index spectrum of ZnSe was directly measured using the self-bending of a pulsed laser beam. It was demonstrated that this effect can provide a simple and reliable method of direct measurement of the nonlinear spectra of semiconductor materials. Self-bending in semiconductors has potential to be used for a new type of efficient nonlinear optical power limiters, in particular for radiation protection of optical sensors and resonatorless optical bistability.

2.v.2. Excitonic nonlinearities in narrow asymmetric coupled quantum wells.

This PI's research group has also been involved in the research related to excitonic nonlinearities in narrow asymmetric coupled quantum wells; the research was motivated by expectations that narrow asymmetric coupled quantum wells as part of SEED devices may under certain circumstances exhibit a blue Stark shift (instead of the regular red one) which might not rely on sharp excitonic transition usually required for the red Stark shift. It was proposed that blue-Stark shift can be achieved by a proper design of asymmetric quantum wells, whereby the first two heavy-hole states in two coupled wells are approaching the resonance. In the experiment [6], a blue shift of the apparent heavy-hole (HH) excitonic transition peak in the photocurrent spectra has been observed, for the first time, in narrow $GaAs/Al_{0.4}Ga_{0.6}As$ asymmetric coupled quantum wells (ACQW's) near the HH pre-resonance. With an external reverse bias of only -2.35 V, a maximum upward shift of the transition energy of ~ 6.1 meV has been measured at 78 K. This blue shift is anomalously large, which cannot be explained by the pre-

anticrossing of HH energy levels in two coupled quantum well. Sharp change of the linewidth of the HH excitonic transitions has also been observed due to the fluctuations in QW's and barrier widths resulting in inhomogeneous broadening of the transitions. CW optical bistability was observed with the external feedback due to this inhomogeneous broadening.

Furthermore, the attempt was made [8] to use all the advantages of the blue shift by attaining an intrinsic feedback mechanism instead of a conventionally used external resistor. This would result in better potential for integration and fabrication of devices. In the experiment [8], strong excitonic nonlinearity in the photoconductive response of a PIN photodiode incorporating narrow asymmetric coupled quantum wells (ACQW's) has been observed at 78 K. When the PIN photodiode is over-biased, the heavy hole (HH) energy levels in the two coupled quantum wells are brought into resonance by increasing the laser intensity. Also, both the light hole (LH) and HH excitonic transitions undergo intensity-dependent shifts. Both of these effects indicate intrinsic change of bias due to redistribution of photogenerated carriers, and therefore, the existence of an intrinsic feedback mechanism. The magnitude of the blue shift of the HH excitonic transitions significantly increases when the laser intensity was changed from $9.2 \ mW/cm^2$ to $\sim 270 \ mW/cm^2$.

2.vi. Other Research

This principal investigator continues to be active in a few areas of nonlinear optics to which he made pioneering contribution (in some of them, like nonlinear interfaces, sixteen years ago). Most recently, he reviewed the most recent research and outlined new research directions on nonlinear optics of a single slightly-relativistic electron [16] (with Y. I. Ding), on bistable solitons and their applications to optical switching [13] in collaboration with R. H. Enns, S. S. Rangnekar of Simon Fraser University (Canada), and on nonlinear interfaces in collaboration with P. Smith and J. Tomlinson of Bellcor [17,18].

3. Work published under AFOSR grant # 90-0180

3.i Regular Journal Papers

[1] D. R. Andersen, D. E. Hooton (U. of Iowa), G. A. Swartzlander (U. of Maryland), and A. E. Kaplan (JHU), "Direct measurements of the transverse velocity of dark spatial solitons", Optics Letters 15: 783-785 (July 15, 1990).

[2] Y. J. Ding, C. L. Guo, G. A. Swartzlander Jr., J. B. Khurgin, and A. E. Kaplan, "Spectral Measurement of the Nonlinear Refractive Index in ZnSe Using Self-Bending of a Pulsed Laser Beam", Opt. Lett. 15: 1431-1433 (Dec. 15, 1990).

[3] C. T. Law and A. E. Kaplan, "Instabilities and amplification of counterpropagating waves in a Kerr nonlinear medium", J. Opt. Soc. Am. B 8: 58-67 (Jan. 1991).

[4] G. A. Swartzlander (JHU), D. R. Andersen, J. J. Regan (U. of Iowa), H. Yin and A. E. Kaplan (JHU), "Spatial dark-soliton stripes and grids in self-defocusing materials", Phys. Rev. Lett. 66: 1583-1585 (25 March 1991).

[5] C. T. Law and A. E. Kaplan, "Dispersion-related amplification in a nonlinear fiber pumped by counterpropagating waves," Opt. Lett. 16: 461-463 (1 April, 1991).

[6] C. L. Guo, Y. J. Ding, S. Li, J. B. Khurgin, C. T. Law, A. E. Kaplan, K.-K. Law, J. Stellato, and L. A. Coldren, "Strong excitonic nonlinearity in a *pin* diode incorporating narrow asymmetric coupled quantum wells," Opt. Lett. 16: 949-951 (15 June, 1991)

[7] P. L. Shkolnikov and A. E. Kaplan, "On the feasibility of X-ray resonant nonlinear effects in plasmas", Opt. Lett. 16: 1153-1155 (1 August, 1991)

[8] Y. J. Ding, C. L. Guo, S. Li, J. B. Khurgin, C. T. Law, A. E. Kaplan, K.-K. Law, J. Stellato, and L. A. Coldren, "Observation of anomalously large blue shift of the excitonic transition and optical bistability in narrow asymmetric coupled quantum wells," Appl. Phys. Lett., 59: 1025-1027 (26 Aug., 1991).

[9] P. L. Shkolnikov and A. E. Kaplan, ""Discharge Plasma - X-ray Laser" resonant couples for X-ray nonlinear optics," Phys. Rev. A, 44: 6951-6953 (15 November, 1991).

[10] P. L. Shkolnikov and A. E. Kaplan, "X-ray third harmonic generation in plasmas of alkali-like ions", Opt. Lett. 16: 1973-1975, (15 December, 1991).

[11] (a) Y. J. Ding and A. E. Kaplan, "Nonlinear magneto-optical effects in vacuum: inhomogeneity-originated second harmonic generation in a dc magnetic field," Intern. J. Nonl. Opt. Phys. 1:51-72 (1992); (2) Y. J. Ding and A. E. Kaplan, Phys. Rev. Lett. 65: 2746 (1990).

[12] P. L. Shkolnikov and A. E. Kaplan, "Proposal for 19.9 nm laser in Li pumped by a non-coherent X-ray pulse" JOSA B 9: 2128-2131 (1992).

[13] R. H. Enns, S. S. Rangnekar (Simon Fraser Univ.), and A. E. Kaplan (JHU), "Optical switching between bistable soliton states: a theoretical review", Optical & Quantum

Electronics, 24: 1295-1314 (1992).

[14] P. L. Shkolnikov, A. E. Kaplan (JHU), and M. H. Muendel and P. L. Hagelstein (MIT), "X-ray laser frequency near-doubling and generation of tunable coherent X-rays in plasma", Appl. Phys. Lett. 61: 2001-2003 (Oct. 1992).

[15] Y. J. Ding and A. E. Kaplan, "Field-gradient-induced second harmonic generation in vacuum", submitted to JOSA B.

3.ii. Books and Book Chapters

[16] A. E. Kaplan and Y. J. Ding, "Nonlinear optics of a single slightly-relativistic electron," invited chapter in the book *"Nonlinear Optics and Optical Computing"*; Eds. S. Martellucci and A. N. Chester, Plenum Press, NY, 1990, pp. 131-147.

[17] A. E. Kaplan, P. W. Smith, and W. J. Tomlinson, "Nonlinear waves and switching effects at nonlinear interfaces", invited chapter in the book *"Nonlinear Waves in Solid State Physics"*, Eds. A. D. Boardman *et al.*, Plenum Press, NY, 1990, pp.93-111.

[18] A. E. Kaplan, P. W. Smith, and W. J. Tomlinson, " Nonlinear Waves and Switching Effects at Nonlinear Interfaces", (invited chapter) in the book "Nonlinear surface electromagnetic phenomena", Eds. H.-E. Ponath and G. I. Stegeman, North-Holland Press, 1991, pp. 323-352.

[19] A. E. Kaplan and P. L. Shkolnikov, "Prospects for X-ray nonlinear optics", in *Nonlinear Optics and Optical Physics* , I. C. Khoo, J. F. Lam, and F. Simoni, eds., World Scientific, to be published.

3.iii. Conference Proceedings

[20] A. E. Kaplan and Y. J. Ding, "Nonlinear magneto-optics of vacuum," (*Invited paper*) STS Press, McLean, VA, 1990, pp. 802-807.

[21] Y. J. Ding, C. L. Guo, G. A. Swartzlander Jr., J. B. Khurgin, and A. E. Kaplan, "Direct measurement of nonlinear refractive index spectrum in ZnSe using self-bending of a pulsed laser beam," STS Press, McLean, VA, 1990, pp. 843-848.

[22] C. T. Law and A. E. Kaplan, "Amplification, instability, and chaos in nonlinear counterpropagating waves," in *Nonlinear Dynamics in Optical Systems,* Eds. N. B. Abraham, E. M. Garmire, and P. Mandell, OSA Proc., v. 7 (Opt. Soc. Am., Washington DC, 1990), pp. 504-508.

[23] P. L. Shkolnikov and A. E. Kaplan, "Saturation-related X-ray resonant nonlinear effects in plasmas", OSA Proceedings on Short Wavelength Coherent Radiation: Generation and Applications, Philip H. Bucksbaum, Natale M. Ceglio, eds. (Optical Society of America, Washington, DC 1991), Vol. 11, pp. 163-166.

[24] D. R. Andersen (U. of Iova), G. A. Swartzlander, Jr. (NRL), A. E. Kaplan (JHU), and S. R. Skinner, G. R. Allan, and A. L. Smirl (U. of Iova), "Dark spatial soliton physics", to appear in SPIE Conf. Proceedings.

[25] A. E. Kaplan and P. L. Shkolnikov, "Frequency upconversion of coherent X-rays by third-order nonlinear optical processes in plasma", Proceedings of LEOS '92 Conference Proceedings (IEEE Lasers and Electro-Optics Society, 1992), pp. 76-77.

[26] P. L. Shkolnikov and A. E. Kaplan, "Resonant frequency transformations of short-wavelength coherent radiation in plasma", OSA Proc. of Short Wavelength V: Physic with Intense Laser Pulses, Eds. P. B. Corkum and M. D. Perry (OSA, Washington, DC, 1993), v. 17, pp. 239-242.

[27] A. E. Kaplan and P. L. Shkolnikov, "Super-dressed two-level atom: very high order harmonic generation and multi-resonances", OSA Proc. of Short Wavelength V: Physic with Intense Laser Pulses, Eds. P. B. Corkum and M. D. Perry (OSA, Washington, DC, 1993), v. 17, pp. 156-158.

3.iv. Conference Papers

[28] A. E. Kaplan, G. A. Swartzlander, and D. R. Andersen, "Spatial dark solitons: discovery and experimental and computer simulation studies", the Workshop "Space-time Complexity in Nonlinear Optics" (March 1990, Tucson, AZ). (*Invited paper)

[29] Y. J. Ding, C. L. Guo, G. A. Swartzlander Jr., J. B. Khurgin, and A. E. Kaplan, "Direct Measurement of Nonlinear Refractive Index Spectrum in ZnSe Using Self-Bending", CLEO'90, Anaheim, CA (May 21-25).

[30] Y. J. Ding and A. E. Kaplan, "Second Harmonic Generation in Magnetized Vacuum", IQEC'90, Anaheim, CA (May 21-25).

[31] G. A. Swartzlander, D. R. Andersen, and A. E. Kaplan, "Dark spatial solitons from amplitude and phase gratings", CLEO'90, Anaheim, CA (May 21-25).

[32] C. T. Law and A. E. Kaplan, "Amplification, instability, and chaos in nonlinear counterpropagating waves," in *Technical Digest Topical Meeting on Nonlinear Dynamics in Optical Systems,* Afton, Oklahoma (June 4-8, 1990).

[33]* A. E. Kaplan, "Relativistic nonlinear optics", at "Nonlinear Optics: Materials, Phenomena and Devices" Conference; (*Invited paper), Kauai, Hawaii, July 16-20, 1990.

[34] C. L. Guo, Y. J. Ding, S. Li, J. B. Khurgin, K.-K. Law, J. Stellato, C. T. Law, and A. E. Kaplan, "Blue-Stark shift of the excitons in optimized asymmetric coupled quantum wells," in *OSA Annual Meeting, 1990, Technical Digest Series, vol. 15* (Optical Society of America, Washington, DC, 1990).

[35] Y. J. Ding, C. L. Guo, J. B. Khurgin, S. Li, K.-K. Law, J. Stellato, A. E. Kaplan, and L. A. Coldren, "Demonstration of optical bistability in narrow asymmetric coupled quantum

wells," 1990 LEOS Ann. Meet., Nov. 4-9, 1990, Boston, Massachusetts, Post Deadline paper, PD15.

[36] Y. J. Ding, C. L. Guo, S. Li, J. B. Khurgin, K.-K. Law, J. Stellato, C. T. Law, and A. E. Kaplan, "Large excitonic optical nonlinearity in optimized asymmetric coupled quantum wells," in *OSA Annual Meeting, 1990, Technical Digest Series, vol. 15* (Optical Society of America, Washington, DC, 1990).

[37]* G. A. Swartzlander, Jr., A. E. Kaplan, and D. R. Andersen, "Optical Self-Bending" (*Invited*) Optical Society of America (OSA) Annual Meeting, Boston, Massachusetts, Nov. 4-9, 1990.

[38] G. A. Swartzlander, Jr., D. R. Andersen, and A. E. Kaplan, "Dark Spatial Solitons Formed By Complex Gratings", Optical Society of America (OSA) Annual Meeting, Boston, Massachusetts, Nov. 4-9, 1990.

[39] P. L. Shkolnikov and A. E. Kaplan. "On the feasibility of X-ray nonlinear effects in plasmas," Conference on Short-Wavelength Coherent Radiation: Generation and Application. April 8-10, 1991, Monterey, California.

[40] C. T. Law and A. E. Kaplan, "Dispersion-related amplification in a lossy nonlinear fiber pumped by counterpropagating waves," Integrated Photonics Research Topical Meeting, Monterey, CA, April 9-11, 1991.

[41]* Andersen, D. R., Swartzlander, G. A., Jr., Kaplan, A. E., Skinner, S. R., Allan, G. R., and Smirl, A. L., "Investigation of Dark Spatial Soliton Phenomena," (*Invited*), Quantum Electronics and Laser Science (QELS'91) Conf., Baltimore, MD, May 1991.

[42] G. A. Swartzlander, Jr., D. R. Andersen, and A. E. Kaplan, "Dark Spatial Soliton (SDS) Filters and Encoders," Conference on Lasers and Electro-Optics (CLEO'91), Baltimore, Maryland, May 12-17, 1991.

[43] Y. J. Ding, C. L. Guo, S. Li, J. B. Khurgin, K.-K. Law, J. Stellato, C. T. Law, A. E. Kaplan, and L. A. Coldren, "Large excitonic blue-shift and nonlinearities in narrow asymmetric coupled quantum wells," 1991 Quant. Optoelectr., Top. Meet., Mar. 11-13, 1991, Salt Lake City, UT; Tech. Dig. Ser. 1991, vol. 7, pp. 78-81, Paper MD6.

[44] Y. J. Ding, C. L. Guo, S. Li, J. B. Khurgin, K.-K. Law, J. Stellato, C. T. Law, A. E. Kaplan, and L. A. Coldren, "Observation of anomalously large excitonic blue shift and optical bistability in narrow asymmetric coupled quantum wells," Conf. on Lasers and Electro-Optics, CLEO'91, May 12-17, 1991, Baltimore, MD.

[45] C. L. Guo, Y. J. Ding, S. Li, J. B. Khurgin, K.-K. Law, J. Stellato, C. T. Law, A. E. Kaplan, and L. A. Coldren, "Evidence of the intrinsic feedback in photocurrent response of *pin* diode incorporating narrow asymmetric coupled quantum wells," Quant. Electr. Laser Science, QELS'91, May 12-17, 1991, Baltimore, MD.

[46] P. L. Shkolnikov and A. E. Kaplan, "X-ray resonant nonlinear optical effects in plasma," Gordon Research Conference on "Nonlinear Optics and Lasers," Wolfeboro, NH, July

22-26 '91.

[47] G. A. Swartzlander, D. R. Andersen, and A. E. Kaplan, "Spatial Dark Solitons," Gordon Research Conference on "Nonlinear Optics and Laser," Wolfeboro, NH, July 22-26 '91.

[48] G. A. Swartzlander Jr., D. R. Andersen, C. T. Law and A. E. Kaplan, "Interaction of (2 + 1)-D spatial dark solitons," in *OSA Annual Meeting,* 1991 OSA Technical Digest Series, vol. 17 (OSA, Washington, DC, 1991).

[49] P. L. Shkolnikov and A. E. Kaplan, "Prospects for X-ray nonlinear optics," OSA 1991 Annual Meeting, Nov. 3-8 '91, San Jose, CA.

[50] P. L. Shkolnikov and A. E. Kaplan, "On the feasibility of X-ray third-harmonic generation in plasmas", OSA 1991 Annual Meeting, Nov. 3-8 '91, San Jose, CA.

[51] G. A. Swartzlander Jr., D. R. Andersen, and A. E. Kaplan, "Spatial dark solitons," "Non-linear Guided-Wave Phenomena" International Topical Meeting; Cambridge, England, Sept. 2-4, 1991.

[52] P. L. Shkolnikov and A. E. Kaplan, "Proposal for VUV laser with X-ray laser resonant pumping," OSA 1991 Annual Meeting, Nov. 3-8 '91, San Jose, CA.

[53] P. L. Shkolnikov and A. E. Kaplan, "On resonant nonlinear interaction of X-ray laser radiation with plasma", OSA 1991 Annual Meeting, Nov. 3-8 '91, San Jose, CA.

[54] P. L. Shkolnikov and A. E. Kaplan, "Proposal for 199 Å X-ray laser in Li", OSA 1991 Annual Meeting, Nov. 3-8 '91, San Jose, CA.

[55] C. T. Law, G. A. Swartzlander, Jr., and A. E. Kaplan, "Propagation dynamics of spatial dark solitons," in *Quantum Electronics and Laser Science Conference,* 1992 OSA Technical Digest Series, v. 13 (Optical Society of America, Washington, DC 1992).

[56] P. L. Shkolnikov and A. E. Kaplan, "X-ray high-harmonic generation: proposals", DAMOP Annual Meeting, May 19-22, '92, Chicago, IL.

[57]* A. E. Kaplan and P. L. Shkolnikov, "Prospects for X-ray nonlinear optics" , I International School on Nonlinear Photonics and Optical Physics, Capri, Italy, June 1-5, 1992 (*Invited paper).

[58]* A. E. Kaplan and P. L. Shkolnikov, "Feasibility of nonlinear optics in the X-ray domain", XVIII International Quantum Electronics Conference, IQEC-92, June 14-19, 1992, Vienna, Austria (*Invited paper).

[59] C. T. Law, G. A. Swartzlander, Jr., and A. E. Kaplan, "Instability of dark soliton stripes," 1992 Annual Meeting of OSA, Albuquerque, 20-25 Sept.'92.

[60] A. E. Kaplan and P. L. Shkolnikov, "Super-dressed two-level system: very high harmonic generation" 1992 Annual Meeting of OSA/ILS-VIII, Albuquerque, 20-25 Sept.'92.

[61] A. E. Kaplan and P. L. Shkolnikov, "Frequency upconversion of coherent X-rays by third-order nonlinear optical processes in plasma", LEOS '92, November 16-19, 1992, Boston, MA.

[62] P. L. Shkolnikov and A. E. Kaplan, "Resonant frequency transformations of short-wavelength coherent radiation in plasma", Short Wavelength V: Physics with Intense Laser Pulses, March 29-31, 1993, San Diego, CA.

[63] P. L. Shkolnikov, A. E. Kaplan, and A. Lago, "Phase matching for large-scale frequency upconversion in plasma", Short Wavelength V: Physics with Intense Laser Pulses, March 29-31, 1993, San Diego, CA.

[64] A. E. Kaplan and P. L. Shkolnikov, "Plateau-cutoff formula for high harmonic generation in two-level atoms", Short Wavelength V: Physics with Intense Laser Pulses, March 29-31, 1993, San Diego, CA.

[65] A. E. Kaplan and P. L. Shkolnikov, "Super-dressed two-level atom: very high order harmonic and combination frequency generation", OSA Annual/ILS-IX, October 3-8, 1993, Toronto, Canada.